PointingSat Case Study

	Name and Function	Date	Signature
Prepared by	**AOCS Team** *TESOA1* *AOCS/GNC Analysis Team*	03.03.2022	
Checked by	**Thomas Ott** *TESOA1* *AOCS/GNC Analyst*	03.03.2022	
Approved by	**Thomas Ott** *TESOA1* *Head of AOCS/GNC & Flight Dynamics*	03.03.2022	
Released by	**Thomas Ott** *TESOA1* Study Lead	03.03.2022	

Summary

PointingSat is a notional geostationary mission for disaster assessment and monitoring of the European continent. The primary payload is a telescope for multi-spectral imaging. The platform is specially developed for the need of the instrument in form of pointing requirements.

This document provides the pointing budget for the performance of telescope of PointingSat. Therefore the mission is analysed towards the error sources affecting the pointing performance of the desired instrument. These Pointing Error Sources (PES) are characterized according to the ESA standard ECSS-E-ST-60-10C and the ESA Pointing Error Engineering Handbook ESSB-HB-E-003. Special focus lay on the modelling possibility of PES in the latest version (V1.1) of the software Pointing Error Engineering Tool (PEET).

This document is structured in the instrument pointing analysis according to the analysis steps within PEET. This case study will be published on the ESA PEET website and in PEET V1.1 as an example for the definition and setup of a pointing system and its evaluation with PEET.

LOG

Document Change Log **P4COM**

Issue/ Revision	Date	Modification Nb	Modified pages	Observations
1/0	31.03.2016		All	Original issue
2/0	18.07.2016		All	
3/0	03.03.2022		All	

Table of Contents

References

APPLICABLE DOCUMENTS

[AD1] ESSB-HB-E-003; ESA Pointing Error Engineering Handbook, Issue 1.0

[AD2] ECSS-E-ST-60-10C; Space Engineering, Control Performance

[AD3] ECSS-E-HB-60-10A; Space Engineering, Control Performance Guidelines

[AD4] IEEE-Std-952-1997 (R2008); IEEE Standard Specification Format Guide and Test Procedure for Single-Axis Interferometric Fiber Optic Gyros

REFERENCE DOCUMENTS

[RD1] Pittelkau M.E., “Pointing Error Definitions, Metrics, and Algorithms”, American Astronautical Society, AAS 03-559, p. 901, 2003.

[RD2] Graf, F.M., Covariance analysis and optimal estimator design, Student Research Project, 2011.

[RD3] Ott T., Benoit A., Van den Braembussche P., Fichter W., “ESA Pointing Error Engineering Handbook”, 8th International ESA Conference on Guidance, Navigation & Control Systems, Karlovy Vary CZ, June 2011.

[RD4] Ott T., Fichter W., Bennani S., Winkler S., "Precision Pointing H_∞ Control Design for Absolute, Window-, and Stability-Time Errors", accepted to be published in CEAS Space Journal.

[RD5] Hirth M., Brandt N., Fichter W., "Inertial Sensing for Future Gravity Missions", GEOTECHNOLOGIEN Science Report No.17, Observation of the System Earth from Space, Bonn, 2010, ISSN: 1619-7399.

[RD6] Hirth M., Fichter W., et al., "Optical Metrology Alignment and Impact on the Measurement Performance of the LISA Technology Package", Journal of Physics Conference Series, 7th International LISA Symposium, Barcelona, Spain, 2008.

[RD7] Hirth M., Ott T., Su H., Pointing Error Engineering Tool – PointingSat Definition, Astos Solutions, 2013

[RD8] Gedon D., Görries S., Systems engineering support to the development of the Pointing Error Engineering SW Framework, GNC_F.TCN.779118.ASTR, 12.01.2016

[RD9] Pittelkau, M.E., McKinley, W.G., “Pointing Error Metrics: Displacement, Smear, Jitter, and Smitter with Application to Image Motion MTF”, AIAA/AAS Astrodynamics Specialist Conference, 13 – 16 Aug 2012, Minneapolis, MN, USA.

[RD10] ESSB-HB-E-003; ESA Pointing Error Engineering Handbook, Issue 1.1 or 2, to be released (ongoing update)

LIST OF ABBREVIATIONS & ACRONYMS

AED	Assembly and Launch Ensemble Domain
AKE	Absolute Knowledge Error
APE	Absolute Performance Error
AST	Analysis Step
CRV	Time-Constant Random Variable
CTF	Coordinate Transformation
EEED	External Environment Ensemble Domain
ENED	Equipment Noise Ensemble Domain
ESA	European Space Agency
FOV	Field Of View
KDE	Knowledge Drift Error
KRE	Knowledge Reproducibility Error
MKE	Mean Knowledge Error
MPE	Mean Performance Error
PDE	Performance Drift Error
PEC	Pointing Error Contributor
PEET	Pointing Error Engineering Tool
PES	Pointing Error Source
PRE	Performance Reproducibility Error
PSF	Point Spread Function
RP	Random Process
RPE	Relative Performance Error
RV	Random Variable

LIST OF SYMBOLS

α	Error on pointing level (rad)
B	Bias (representing CRV)
BM(A)	Bimodal PDF with Amplitude A
Δ	Discrete distribution
$\varepsilon_D(D, \Delta t_D)$	Drift type PES with slope D and time span Δt_D
$G(\mu,\sigma^2)$	Gaussian PDF with mean μ and variance σ^2
N	Random process type PES in terms of PSD
P(f,A)	Periodic type PES with frequency f and amplitude A
T(t)	Time series
$U(e_{min}, e_{max})$	Uniform PDF between $\mathbf{e}_{min}$ and $\mathbf{e}_{max}$

1 Introduction

This document contains the definition of the PointingSat used within the PEET project. PointingSat describes an artificial precision pointing satellite mission with typical pointing error sources and system transfers. It serves as an example for a possible application of the methodology described in the ESA Pointing Error Engineering Handbook [AD1]/[RD10] concerning the setup interpretation of pointing error sources and how to realize this methodology with the PEET software. Models and typical parameters are to a large extent based on inputs provided by ESA and [RD3]-[RD6].

This document has been updated by Airbus DS for the ESA study “P4Com" performed by ASTOS Solutions and as a subcontractor by Airbus DS. It bases on the original PointingSat definition document for the prototype versions of PEET, [RD7]. Extensions of this example for the enhanced functionalities of PEETv1.1beta are included in this document.

2 PointingSat Specification and Requirements

2.1 'Functional Requirements'

This section briefly summarizes general topics which shall be covered by the PointingSat example.

2.1.1 PES Representation

The set of PES for the PointingSat example shall cover at least one of the following representations:

- Time-constant random variables
- Periodic errors
- Transient errors (general periodic signals)
- Random processes characterized by:
  - Band-limited white noise
  - Power spectral densities
- Time-random variables
- Drifts

2.1.2 Ensemble-Domain Definition

Not all PES of PointingSat arise from the same physical background. Hence, at least two ensemble-domains shall be included. Each PES has to be assigned to one of these domains for the correct evaluation.

2.1.3 Statistical Interpretation

The PointingSat example PES shall cover the following statistical interpretation types for the ensemble-domains:

- Worst-case interpretation
- Statistical interpretation

The statistical interpretation for the temporal-domain shall cover the following statistical interpretation type:

- Worst-case interpretation
- Statistical interpretation

Note: A worst-case interpretation of the temporal-domain in combination with a worst-case ensemble-domain interpretation is physically not useful and thus this case shall not be included in the PointingSat example.

2.1.4 Pointing Error Index

The system pointing error requirements of PointingSat shall be characterized by:

- Dependency on instantaneous time only (e.g. AKE, APE)
- Dependency on a window time (e.g. MKE, MPE, RKE, RPE, WPD, WPR)
- Dependency on a stability time (e.g. KDE, KRE, PDE, PRE)

2.1.5 Correlation

The PointingSat example PES shall account for the following correlation setting for each ensemble-domain:

- Between different random variable described PES (arbitrary correlation in range [-1;1])
- Between different random process described PES (arbitrary coherence in range [0;1])
- Between different periodic described PES (via arbitrary phase setting in range [0;2π[)
- Between the ensemble-parameter of one ensemble-domain (arbitrary correlation in range [-1;1])

2.1.6 System Transfer

The transfer from the PES of the PointingSat example to PEC shall at least be realized using the following system representations:

- Static system (e.g. coordinate transformation)
- Dynamic system (e.g. transfer functions)
- Summation of PES
- Container

2.1.7 Post Processing

The PointingSat example shall include a post processing script at least on the total error.

2.2 Mission and System Specification

PointingSat is a geostationary mission supporting the disaster assessment and monitoring for the European continent. The primary payload is a telescope for multi-spectral imaging (VIS, NIR, TIR, and MW) which allows detection and tracking of different ecological, economical and humanitarian incident follow-ups such as fires, algal bloom spread, oil slick or infrastructural damages after earthquakes, floods or windstorms. The mission is illustrated in Figure 2-1.

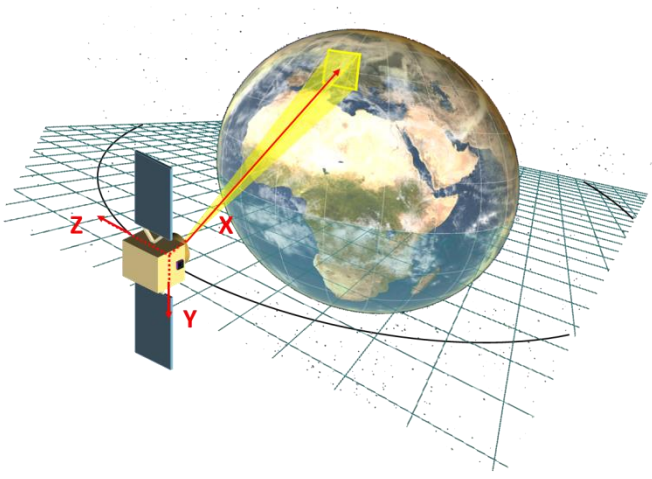

Figure 2-1: Representation of PointingSat Mission

As (dependent on the incident to be observed) the areas to be monitored are much larger than the payload FOV, highly accurate pointing and pointing stability of the satellite is required to allow single

raster scanning of the relevant area on the one hand and repeated scanning of the same area in different spectral ranges.

Above mentioned image acquisition strategy and multi-channel usage leads to requirements on different kinds of pointing errors (error indices), APE, PDE and RPE, whose general definitions are illustrated in Figure 2-2 below. The RPE can be further separated into a linear drift WPD that leads to a smear over the sensor pixels, and the remaining residual error WPR, that leads to widening of the point spread function. Figure 2-3 below.

As mentioned above, the main payload of PointingSat is a high-resolution telescope which is mounted on an ultra-stable optical bench. The IR focal planes are housed in cryostats and cooled by mechanical cryocoolers.

The PointingSat AOCS uses a star-tracker (2 camera heads in cold redundancy) and fibre-optical gyros (3+3 cold-redundant) for attitude and rate determination. A set of 5 reaction wheels is used for the pointing attitude manoeuvres.

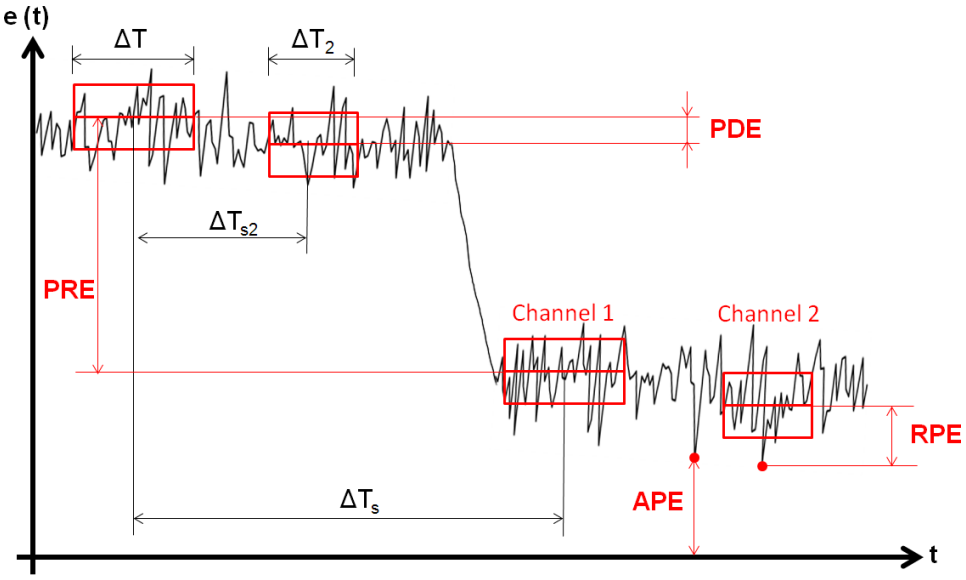

Figure 2-2: Different relevant error indices for PointingSat

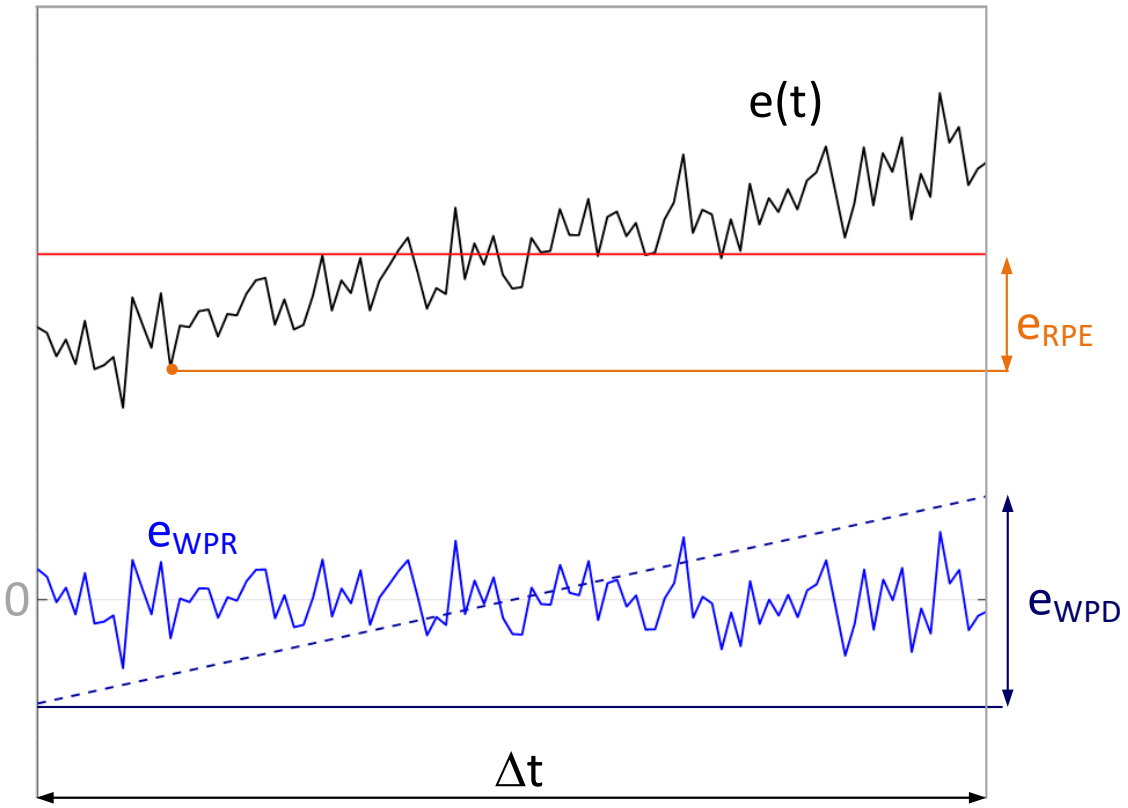

Figure 2-3: RPE, WPD and WPR for PointingSat

2.3 Pointing Error Requirements

To achieve the mission objectives of PointingSat within the targeted accuracy, the following requirements on the system pointing error have to be met:

- **APE**

As the mission objective is disaster monitoring, the main objective is to point during one entire observation period at the correct scene with a probability Pc. This requirement is driven by 'geo-location', i.e. images are acquired from the correct pointing scene of interest in order to reliably detect disasters.

This requires the application of the chosen domain treatment to ensure that the pointing error during one entire (100 % of time) observation k is less than the defined LoS error eAPE,req.

Table 2-1: PointingSat APE Requirement

Pointing Error Requirement (PER)		Absolute Performance Error (APE)				Comments
Evaluation Period		One observation period				common LoC evaluation
Error Index		APE				
Window-Time [s]		-				
Stability-Time [s]		-				
Unit		arcsec				
Required Error Value		X	y	z	LoS	
					150	
Ensemble Domains		Pc				
'Assembly+Launch' Ensemble (AED) 'Equipment Noise' Ensemble (ENED) 'External Environment' Ensemble (EEED)		99.7%				
'Station Keeping Manoeuvre' Ensemble (SKM)						
Domain Treatment		Temporal Domain				
		Statistical			Worst-case	
Ensemble Domain	Statistical	-			AED, ENED, EEED, SKM	
	Worst-case	-			-	
Error reference frame		LoS (x-axis) of the PointingSat-SAT-S frame				
Applied PES		All				

- **RPE**

This requirement is driven by the need of a stable orientation throughout the integration time of the respective spectral channel (the window time Δt represents the maximum integration time out of the individual channels). The image quality is determined by the aberration of the point spread function (PSF) during the integration time of a single observation [RD1]. Pointing variations during exposure lead to a broadening of the point spread function and thus to a reduction of the signal to noise ratio (SNR). A linear drift over the exposure time can lead to errors in the reconstruction of the PSF centroid. Therefore, the RPE requirement is split into a Windowed Performance Drift (WPD) and the remaining Windowed Performance Residual (WPR). Those correspond to Smear and Jitter in [RD1].

Table 2-2: PointingSat RPE Requirement

Pointing Error Requirement (PER)	**Relative Performance Error (RPE)**				**Comments**
Evaluation Period	One observation period				individual LoC evaluation
Error Index	RPE				
Window-Time [s]	1				
Stability-Time [s]	-				
Unit	arcsec				
Required Error Value	X	y	z	LoS	
				8	
Ensemble Domains	Pc				
'Assembly+Launch' Ensemble (AED)	95.5%				
'Equipment Noise' Ensemble (ENED)	68.2%				
'External Environment' Ensemble (EEED)	68.2%				
'Station Keeping Manoeuvre' Ensemble (SKM)	68.2%				
Domain Treatment	Temporal Domain				
	Statistical			Worst-case	
Ensemble Domain – Statistical	-			-	
Ensemble Domain – Worst-case	AED, ENED, EEED, SKM			-	
Error reference frame	LoS (x-axis) of the PointingSat-SAT-S frame				
Applied PES	All				

This error not only degrades the image quality, the raster/mosaic scan is affected as well. Pointing variations ε_{RPE} during exposure lead to a narrowing of the effective field of view as areas at the edge of the image are not covered at all time. Consequently the nominal image size h_{nom} is reduced to an effective image size h_{eff} and gaps between adjacent images may occur. This is illustrated in Figure 2-4 below.

As it has to be ensured that the RPE requirement is met for at least a fraction P_c of the overall integration time with 100% probability for sufficient image quality, temporal-domain statistical and ensemble-domain worst-case interpretation applies in this case.

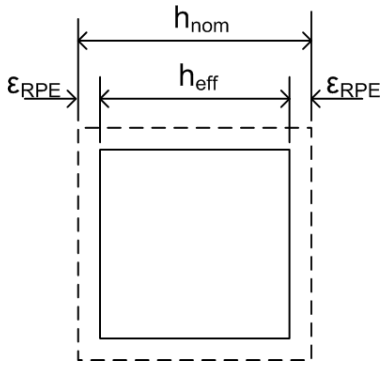

Figure 2-4: Impact of RPE on effective images size

Note: Instead of computing the mean variance of the relative error w.r.t the mean value of the time window, the instantaneous relative error at a defined point t within the time window can sometimes be of interest. This is possible in PEET and reflected in the PointingSat example with the RPE_gamma for comparison to the 'normal' RPE, but shall not be further discussed in this example. Please refer to the PEET user manual for further information.

As mentioned in the beginning of this chapter, the RPE requirement can be further broken down into a linear drift component and the remaining residual error. This is reflected by the WPD and WPR requirements below. The linear drift component leads to smear on the imaging sensor and thereby deformation of the point spread function. Under the assumption of a Gaussian distribution, the remaining residual error leads only to a widening of the point spread function. This causes a reduction of the signal to noise ratio, but does not affect the reconstruction of the point spread function centroid.

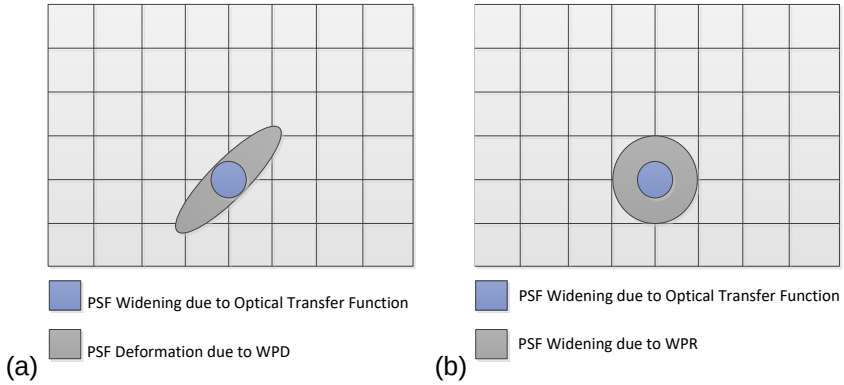

Figure 2-5: Deformation (a) and widening (b) of the point spread function through WPD and WPR

Table 2-3: PointingSat WPD Requirement

Pointing Error Requirement (PER)		Windowed Performance Drift Error (WPD)				Comments
Evaluation Period		One observation period				individual LoC evaluation
Error Index		WPD				
Window-Time [s]		1				
Stability-Time [s]		-				
Unit		arcsec				
Required Error Value		X	y	z	LoS	
					5	
Ensemble Domains		Pc				
'Assembly+Launch' Ensemble (AED)		95.5%				
'Equipment Noise' Ensemble (ENED)		68.2%				
'External Environment' Ensemble (EEED)		68.2%				
'Station Keeping Manoeuvre' Ensemble (SKM)		68.2%				
Domain Treatment		Temporal Domain				
		Statistical			Worst-case	
Ensemble Domain	Statistical	-			-	
	Worst-case	AED, ENED, EEED, SKM			-	
Error reference frame		LoS (x-axis) of the PointingSat-SAT-S frame				
Applied PES		All				

Table 2-4: PointingSat WPR Requirement

Pointing Error Requirement (PER)		Windowed Performance Residual Error (WPR)				Comments
Evaluation Period		One observation period				individual LoC evaluation
Error Index		WPR				
Window-Time [s]		1				
Stability-Time [s]		-				
Unit		arcsec				
Required Error Value		X	y	z	LoS	
					7	
Ensemble Domains		Pc				
'Assembly+Launch' Ensemble (AED)		95.5%				
'Equipment Noise' Ensemble (ENED)		68.2%				
'External Environment' Ensemble (EEED)		68.2%				
'Station Keeping Manoeuvre' Ensemble (SKM)		68.2%				
Domain Treatment		Temporal Domain				
		Statistical			Worst-case	
Ensemble Domain	Statistical	-			-	
	Worst-case	AED, ENED, EEED, SKM			-	
Error reference frame		LoS (x-axis) of the PointingSat-SAT-S frame				
Applied PES		All				

- **PDE**

This requirement is driven by the need of a proper orientation between adjacent images of the scanning raster in case the target area cannot be covered by the telescope field of view. The window time ΔT depicts the time needed for one recording. The stability time ΔT_s represents the total time required for one observation cycle, i.e. to achieve the full mosaic image.

Table 2-5: PointingSat PDE Requirement

Pointing Error Requirement (PER)		**Performance Drift Error (PDE)**				**Comments**
Evaluation Period		One observation period				individual LoC evaluation
Error Index		PDE				
Window-Time [s]		1				
Stability-Time [s]		600				
Unit		arcsec				
Required Error Value		X	y	z	LoS	
					50	
Ensemble Domains		Pc				
'Assembly+Launch' Ensemble (AED)		99.7%				
'Equipment Noise' Ensemble (ENED)		99.7%				
'External Environment' Ensemble (EEED)		99.7%				
'Station Keeping Manoeuvre' Ensemble (SKM)		99.7%				
Domain Treatment		Temporal Domain				
		Statistical			Worst-case	
Ensemble Domain	Statistical	AED, ENED, EEED, SKM			-	
	Worst-case	-			-	
Error reference frame		LoS (x-axis) of the PointingSat-SAT-S frame				
Applied PES		All				

If a raster of N x M pictures is assumed (compare Figure 2-6), ΔT_s can be derived from:

$$\Delta T_s = N \cdot M \cdot \left(T_{slew} + T_{channels}\right) - T_{slew} \qquad \text{Eq 2-1}$$

where T_{slew} is the time required for the spacecraft reorientation to the next pointing scene and $T_{channels}$ represents the total time required for the image acquisition on all channels for one pointing scene[1].

The effect of the PDE can be illustrated as follows: Assume the nominal size of the field of view for one raster image is given by h_{nom} and a slew $d_{nom} = h_{nom}$ is commanded between each of the different pointing scenes. Then - dependent on its direction - a line of sight error motion of the first image (point spread function centroid) with respect to all other images (point spread function centroids) can result in gaps (black areas in Figure 2-6) or overlaps (dashed areas in Figure 2-6) between images.

In case of the PDE the statistical interpretation applies for the temporal- and the ensemble-domain as both behaviours are of interest.

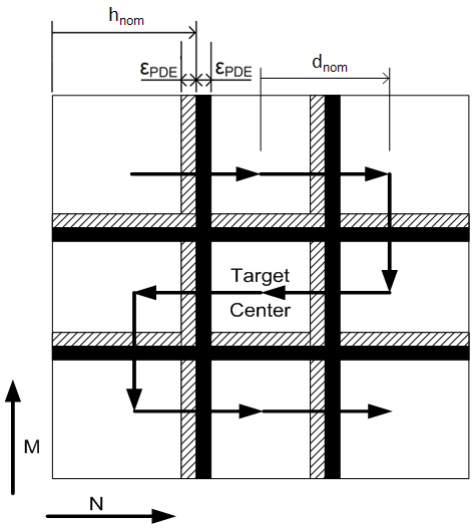

Figure 2-6: Impact of PRE on raster pointing sequence

- **AKE**

The absolute knowledge error is defined as spectral requirement. The only PES that contribute to this error index are the ones, influencing the gyro stellar estimator model as well as thermal deformations between star tracker reference frame and payload.

There are two output signals of the gyro stellar estimator: The estimated rate error ω_{est} and the estimated attitude error φ_{est}. The attitude estimation error is combined with the thermal deformations. The overall contribution PSD has to fit the following PSD as depicted in Figure 2-7 and given in by the following transfer function shaping filter:

$$e_{\mathrm{AKE,spectral}} \leq e_{\mathrm{AKE,spectral,req}} = \begin{cases} \frac{100s+100}{s^2+10.1s+1} & x,y\text{-axis} \\ \frac{75s+75}{s^2+10.1s+1} & z\text{-axis} \end{cases} \qquad \text{Eq 2-2}$$

The spectral requirement of the attitude and bias error are depicted as a PSD in Figure 2-7.

[1] Note that generally another PDE requirement exists related to a stability time ΔT_{s2} (not treated here). This stability time corresponds to the adjustment/processing time between an acquisition of the same pointing scene on different channels. The respective window time ΔT_2 is then the same as the minimum window time ΔT of all channels.

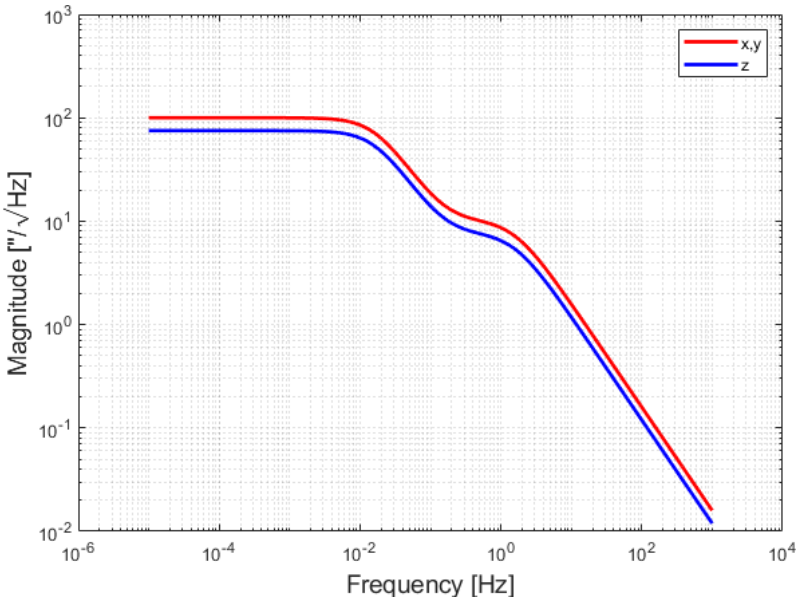

Figure 2-7: $e_{AKE,spectral,req}$

2.4 Coordinate Frames

2.4.1 Franck Diagram

The following Franck diagram in Figure 2-8 illustrates the transformation chain of the different coordinate frames used for the pointing assessment of PointingSat. The coordinate frames are further illustrated and explained in the subchapters following thereafter.

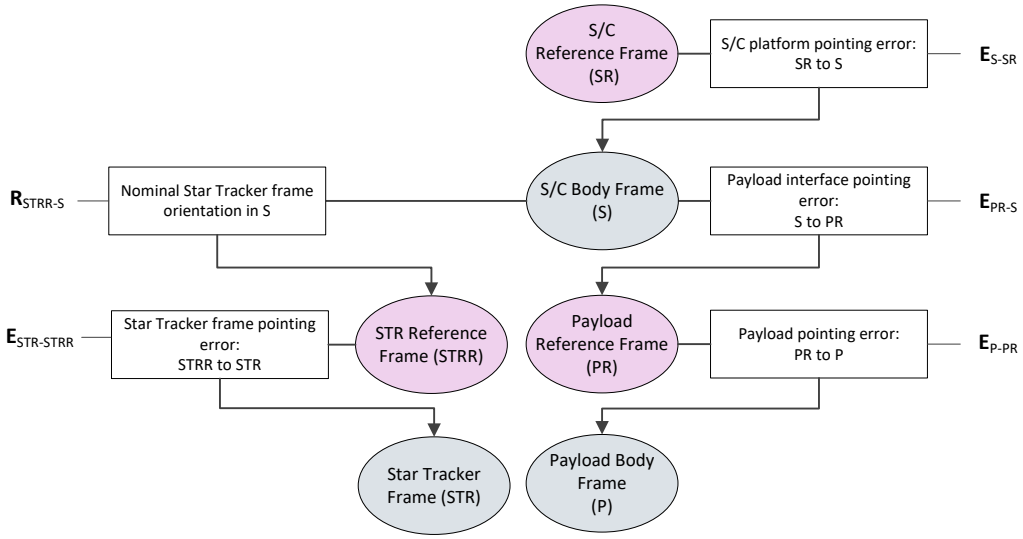

Figure 2-8: Franck Diagram with PointingSat Reference Frames

2.4.2 S/C Reference Frame

2.4.2.1 Overview

Name	Type	Mnemonic	ID
Geodetic Local Normal Reference Frame	Orbital	SR	PointingSat-ORB-LN

The PointingSat S/C reference frame is the Geodetic Local Normal reference frame. This frame is an orbital frame that is orthogonal, right-handed.

2.4.2.2 Definition

$REF_{SR} = \{O_{SR}; X_{SR}, Y_{SR}, Z_{SR}\}$:

- The origin O_{SR} is located in the nominal S/C centre of mass
- X_{SR}: parallel to the local normal of the Earth reference ellipsoid at the sub-satellite point, i.e. Geodetic Nadir pointing downwards from the satellite towards the Earth surface;
- Y_{SR}: anti-parallel the satellite orbital angular momentum;
- Z_{SR}: completes the ortho-normal, right-handed reference frame: $X_{SR} = Y_{SR} \times Z_{SR}$;

2.4.2.3 Diagram

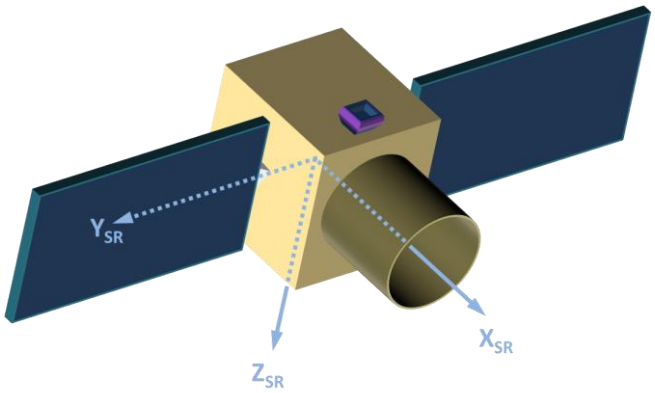

Figure 2-9: PointingSat Reference Frame

2.4.3 S/C Body Frame

2.4.3.1 Overview

Name	Type	Mnemonic	ID
S/C Body Frame	Satellite fixed	S	PointingSat-SAT-S

The PointingSat S/C body frame is identical with the PointingSat reference frame. Furthermore it is identical to the mechanical reference frame and the principal axis frame. This frame is a satellite fixed frame that is orthogonal, right-handed.

2.4.3.2 Definition

$REF_S = \{O_S; X_S, Y_S, Z_S\}$:

- The origin O_S is located in the nominal S/C centre of mass
- X_S, Y_S and Z_S are identical to X_{SR}, Y_{SR} and Z_{SR}

2.4.3.3 Diagram

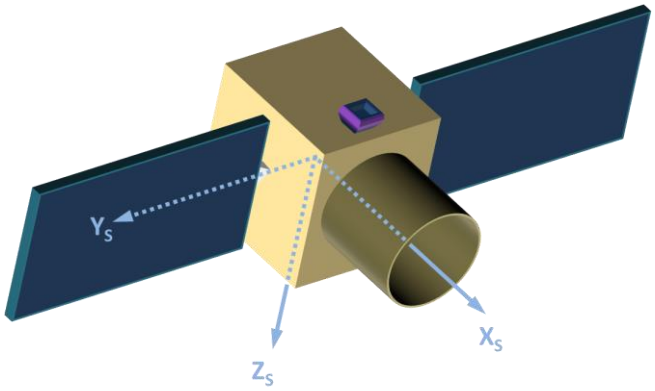

Figure 2-10: PointingSat Body Reference Frame

2.4.4 Payload Reference Frame

2.4.4.1 Overview

Name	Type	Mnemonic	ID
Payload Reference Frame	Satellite fixed	PR	PointingSat-SAT-PR

The PointingSat payload reference frame is defined for the optical payload for the S/C. This frame is an satellite frame that is orthogonal, right-handed.

2.4.4.2 Definition

$REF_{PR} = \{O_{PR}; X_{PR}, Y_{PR}, Z_{PR}\}$:

- The origin O_{PR} is located on the mounting plane of the payload. The origin shall be one of the payload mounting feet.
- X_{PR}: is parallel to and oriented like X_S;
- Y_{PR}: is parallel to and oriented like Y_S;
- Z_{PR}: is the observation axis and is parallel and oritented like Z_s

2.4.4.3 Transformation

from PointingSat-SAT-S *to* PointingSat-SAT-PR

Translation: A distance equal to the distance from the origin of REF_S to the origin of REF_{PR}.

Rotation: none

2.4.4.4 Formula

$$\begin{bmatrix} x \\ y \\ z \end{bmatrix}_{PR} = \begin{bmatrix} x \\ y \\ z \end{bmatrix}_{S} - \begin{bmatrix} r_x \\ r_y \\ r_z \end{bmatrix}_{PR,S} \qquad \text{Eq 2-3}$$

where $(r_x,r_y,r_z)_{PR,S}$ is the position of the origin O_{PR} of the Payload Reference Frame in the Satellite Body Frame.

2.4.4.5 Diagram

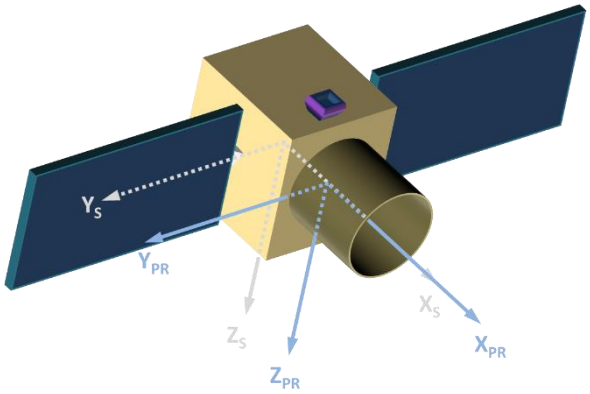

Figure 2-11: PointingSat Payload Reference Frame

2.4.5 Payload Body Frame

2.4.5.1 Overview

Name	Type	Mnemonic	ID
Payload Body Frame	Satellite fixed	P	PointingSat-SAT-P

The PointingSat payload body frame is defined for the internal axes of the optical payload for the S/C. This frame is an payload fixed frame that is orthogonal, right-handed.

2.4.5.2 Definition

$REF_P = \{O_P; X_P, Y_P, Z_P\}$:

- The origin O_P is located in the focal plane of the optical instrument
- X_P, Y_P and Z_P: are aligned with REF_{PR}, where Z_P is the observation axis;

2.4.5.3 Diagram

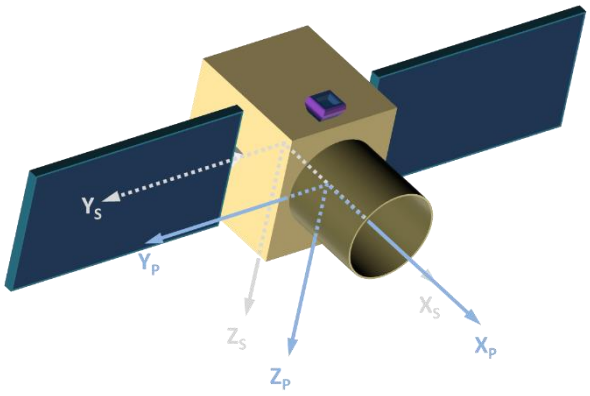

Figure 2-12: PointingSat Payload Body Frame

2.4.6 Star Tracker Frame

2.4.6.1 Overview

Name	Type	Mnemonic	ID
Star Tracker Frame	Satellite fixed	STR	PointingSat-SAT-STR

The PointingSat star tracker frame is defined for the internal axes of the star tracker of the S/C. This frame is an satellite fixed frame that is orthogonal, right-handed.

2.4.6.2 Definition

REF_{STR} = {O_{STR}; X_{STR}, Y_{STR}, Z_{STR}}:

- The origin O_{STR} is located in the detector plane of the star tracker
- X_{STR}: completes the system to a right-handed system
- Y_{STR}: anti-parallel to Z_S
- Z_{STR}: is the boresight axis and parallel to X_S

2.4.6.3 Transformation

from PointingSat-SAT-S *to* PointingSat-SAT-STR

Translation: A distance equal to the distance from the origin of REF_S to the origin of REF_{STR}.

Rotation: Around X_S and Y_S.

2.4.6.4 Formula

$$\begin{bmatrix} x \\ y \\ z \end{bmatrix}_{STR} = \mathbf{R}_z(-90°)\mathbf{R}_y(180°)\left(\begin{bmatrix} x \\ y \\ z \end{bmatrix}_S - \begin{bmatrix} r_x \\ r_y \\ r_z \end{bmatrix}_{STR,S}\right) \quad \text{Eq 2-4}$$

where $(r_x,r_y,r_z)_{STR,S}$ is the position of the origin O_{STR} of the star tracker body frame in the satellite body frame.

2.4.6.5 Diagram

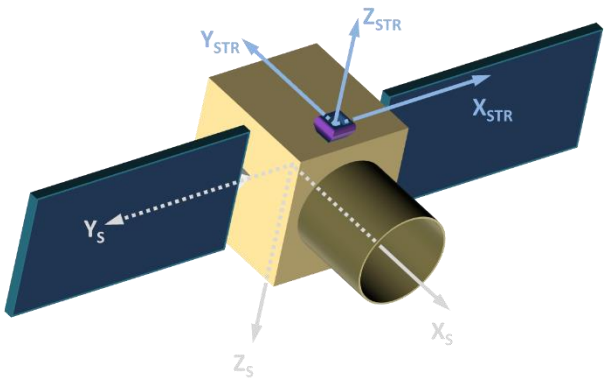

Figure 2-13: PointingSat Star Tracker Frame

3 Characterization of PES (AST-1)

The following subchapters describe in detail the definition of the PES which affect the pointing performance of PointingSat. This description includes information about modelling and the statistical interpretation.

The described PES can be roughly categorized as follows:

- Integration/Assembly errors: PES 1 and PES 2
- Actuator errors: PES 4
- Sensor errors:
  - Star tracker: PES 3, PES 5 and PES 6
  - Gyro: PES 7
- Environmental errors: PES 8 – PES 17
- Manoeuvre related errors: PES 18

These PES are assigned to four different ensemble-domains due to their common physical backgrounds:

- Ensemble-Domain 1: Assembly and Launch PES 1 – PES 3
- Ensemble-Domain 2: Equipment Noise PES 4 – PES 8
- Ensemble-Domain 3: External Environment PES 9 –PES 17
- Ensemble-Domain 4: Station Keeping Manoeuvre PES 18

3.1 Ensemble-Domain 1: Assembly and Launch

The 'Assembly+Launch' ensemble domain is related to errors that are random with respect to assembly and launch effects such as misalignments, settling effects, etc. After building and launching one satellite out of the ensemble of possible satellites, these errors are considered to be constant over the whole mission lifetime.

3.1.1 PES 1: Mechanical Payload and Star Tracker Alignment

3.1.1.1 Description

This PES represents the misalignment error knowledge between the payload axes and the star tracker axis expressed in the satellite body reference frame. Due to limitations of the manufacturing process itself, positioning of the payload telescope and the star tracker is only feasible within certain mechanical tolerances. Once assembled, a fixed misalignment error is present which is determined via theodolite measurements (and which can be compensated for in post-processing). However, the measuring device itself is also limited in its accuracy.

3.1.1.2 Model

Due to its time-constant property the PES is modelled as CRV. By the theodolite measurement device for the determination of the misalignment the error is assumed to be Gaussian distributed with certain limitations. Therefore it is modelled as zero-mean truncated Gaussian error.

PES1 Model	
Type	Random Variable
Class	Bias
Time-Random	no
Ensemble-Random	yes
Ensemble Domain	Assembly and Launch
Physical unit	[arcsec]
Temporal Distribution	Discrete
Ensemble Distribution	Truncated Gaussian
Parameter	$\boldsymbol{\alpha}_1 = \begin{bmatrix} \delta\left(G_t(0,\sigma_{1,x}^2,-\alpha_{1,\max,x},\alpha_{1,\max,x})\right) \\ \delta\left(G_t(0,\sigma_{1,y}^2,-\alpha_{1,\max,y},\alpha_{1,\max,y})\right) \\ \delta\left(G_t(0,\sigma_{1,z}^2,-\alpha_{1,\max,z},\alpha_{1,\max,z})\right) \end{bmatrix} = \begin{bmatrix} \delta\left(G_t(0,10^2-27,27)\right) \\ \delta\left(G_t(0,8^2-22,22)\right) \\ \delta\left(G_t(0,9^2-23,23)\right) \end{bmatrix}$

where $\alpha_{1,max,ax}$ describes the maximum knowledge error of the measurement process on axis ax).

3.1.2 PES 2: Star Tracker to Payload Alignment after Launch

3.1.2.1 Description

This PES represents the alignment error between the star tracker axes and the payload axis resulting from the launch of the satellite. This misalignment arises first from distortions of the structure due to the transfer from 1g to 0g environment and second from permanent distortion induced by the vibration loads during the launch. However, once in orbit, this error remains constant over time.

3.1.2.2 Model

The PES is time-constant and numerous different structural elements might be subject to the distortions. According to this presetting, the PES can be modelled as zero mean CRV with Gaussian ensemble distribution:

PES2 Model	
Type	Random Variable
Class	Bias
Time-Random	no
Ensemble-Random	yes
Ensemble Domain	Assembly and Launch
Physical unit	[arcsec]
Temporal Distribution	Discrete
Ensemble Distribution	Gaussian
Parameter	$\boldsymbol{\alpha}_2 = \begin{bmatrix} \delta\left(G(0,\sigma_{2,x}^2)\right) \\ \delta\left(G(0,\sigma_{2,y}^2)\right) \\ \delta\left(G(0,\sigma_{2,z}^2)\right) \end{bmatrix} = \begin{bmatrix} \delta\left(G(0,15^2)\right) \\ \delta\left(G(0,10^2)\right) \\ \delta\left(G(0,5^2)\right) \end{bmatrix}$

where $\sigma_{2,ax}$ describes the standard deviation of the error on the respective axis ax.

3.1.3 PES 3: Star Tracker Bias

3.1.3.1 Description

This PES represents the bias error knowledge of the star tracker measurement axes with respect to the nominal star tracker frame. It combines the contributions of on-ground calibration residuals and launch effects. Once in orbit, a fixed bias error is present.

3.1.3.2 Model

The PES is described in the PointingSat-SAT-STR reference frame. It is time-constant and the probability of obtaining a bias error within a given accuracy range of the calibration process is equal. The same is assumed for the launch effect contribution at this point. Thus, it is modelled as zero mean CRV with uniform distribution:

PES3 Model	
Type	Random Variable
Class	Bias
Time-Random	no
Ensemble-Random	yes
Ensemble Domain	Assembly and Launch
Physical unit	[arcsec]
Temporal Distribution	Discrete
Ensemble Distribution	Uniform
Parameter	$\boldsymbol{\alpha}_3 = \begin{bmatrix} \delta\left(U(0,\alpha_{3,\max,x})\right) \\ \delta\left(U(0,\alpha_{3,\max,y})\right) \\ \delta\left(U(0,\alpha_{3,\max,z})\right) \end{bmatrix} = \begin{bmatrix} \delta\left(U(0,8)\right) \\ \delta\left(U(0,8)\right) \\ \delta\left(U(0,7)\right) \end{bmatrix}$

where $\alpha_{3,max,ax}$ describes the maximum error of the measurement process on axis ax and z represents the boresight axis of the star tracker.

3.2 Ensemble-Domain 2: Equipment Noise

Each sensor and actuator mounted on PointingSat has a certain level of noise. This is summarized in the 'Equipment Noise' ensemble domain. Therefore their effect can be evaluated in the same manner as these errors basically influence the performance in the same way.

3.2.1 PES 4: Reaction Wheel Friction Steps and Spikes

3.2.1.1 Description

This PES represents the disturbance torque transients induced by friction steps and spikes in one individual reaction wheel. PointingSat uses an array of five of identical reaction wheels in a pyramid configuration for attitude control.

The disturbance torque acts around the reaction wheel axis of the individual actuator frame. Assume that it has been characterized by the manufacturer in test facilities and in-orbit data. The figure below illustrates the characteristics of the transient behaviour in the time domain as well as the Fourier series approximation used to model it in PEET.

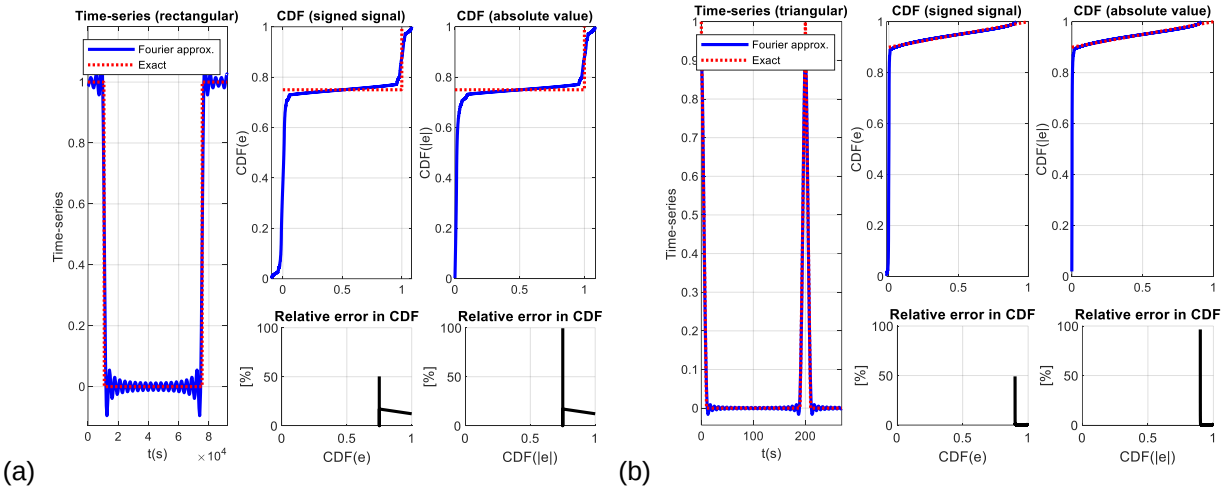

Figure 3-1: Reaction wheel torque transients due to friction steps (a) and spikes (b)

3.2.1.2 Model

Assume that - given the characteristics from the datasheet - the PES can be modelled as:

PES4 Steps Model	
Type	Transient (General Periodic Signal)
Class	Rectangular
Time-Random	no
Ensemble-Random	no
Ensemble Domain	Equipment Noise
Physical unit	[Nm]
Temporal Distribution	
Ensemble Distribution	-
Parameter	Fundamental period 1 s On-Off ratio: 25 % Amplitude: 0.005 Nm

PES4 Spikes Model	
Type	Transient (General Periodic Signal)
Class	Triangular
Time-Random	no
Ensemble-Random	no
Ensemble Domain	Equipment Noise
Physical unit	[Nm]
Temporal Distribution	
Ensemble Distribution	-
Parameter	Fundamental period 200 s On-Off ratio: 10 % Amplitude: 0.013 Nm

Above definition implies an ideal torque realization in the desired direction and only ‘one-dimensional’ information is required. In case RW misalignment errors (more precisely the knowledge of these errors) should be taken into account, generally two options exist:

- The error is defined by a one-dimensional PES for the torque direction only. The misalignment and displacement of each RW can individually be adapted by modifying the respective part in the actuation matrix (first block in Figure 4-4).
- The PES is already defined in terms of a resulting torque noise (after taking into account all individual displacements and misalignments in the actuation matrix that lead to a worst case torque noise on body axes) and the actuation matrix transfer is omitted.

All above options are supported by PEET, once the user has carried out the required calculations outside PEET. Indeed, the worst case of the torque noise on body axes depends on the design of the actuation concept (number, position and orientation of RWs). The identification of this worst case is outside the scope of PEET. Within this example the first listed solution with an actuation matrix is chosen.

3.2.2 PES 5: Star Tracker Noise (Temporal)

3.2.2.1 Description

This PES represents the unprocessed attitude errors related to internal temporal noise of the star tracker unit such as read-out noise and quantization noise. This part of the noise is considered as independent of the operational conditions (e.g. temperature, star pattern in field of view). The error information for the different axes (around/across boresight) of this PES in the sensor frame is taken from the data sheet of the manufacturer. The data sheet provides the errors in the form of standard deviations of a random process for the across-boresight axes (x,y) and the around-boresight axis (z) together with a corresponding sampling time.

3.2.2.2 Model

The PES is described in the PointingSat-SAT-STR reference frame. With the information from the description, the PES will be of RP type described by a band-limited white noise, i.e.

PES5 Model	
Type	Random Process
Class	Random
Time-Random	yes
Ensemble-Random	no
Ensemble Domain	Equipment Noise
Physical unit	$[\text{arcsec}/\sqrt{\text{Hz}}]$
Temporal Distribution	Gaussian
Ensemble Distribution	-
Parameter	$PSD_5 = \begin{bmatrix} PSD_{5,xx} \\ PSD_{5,yy} \\ PSD_{5,zz} \end{bmatrix}$ Defined by the band-limited white noise: $\text{cov}_5 = \begin{bmatrix} \sigma_{5,c}^2 \\ \sigma_{5,c}^2 \\ \sigma_{5,a}^2 \end{bmatrix} = \begin{bmatrix} 1.2^2 \\ 1.2^2 \\ 8^2 \end{bmatrix} \text{arcsec}^2$ And the sampling time $f_{sampling} = 8Hz$

where $\sigma_{5,c}$ describes the across-boresight standard deviation and $\sigma_{5,a}$ the standard deviation around boresight. PSD_5 is displayed in vector form for compactness, as the non-diagonal entries are zero. Equal applies to cov_5 as these values define the PSD_5.

Note that in PEET this representation is converted to an equivalent PSD with white noise behaviour up to a cut-off frequency which corresponds to the Nyquist frequency of the given sampling time. An equivalent expression of above described PES is given by Figure 3-2:

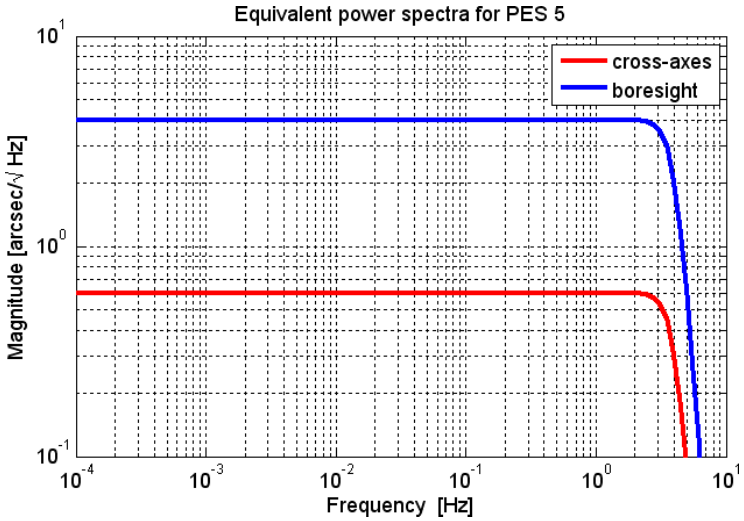

Figure 3-2: Equivalent temporal star tracker noise PSD

3.2.3 PES 6: Star Tracker FOV and Pixel Spatial Errors

3.2.3.1 Description

This PES represents the unprocessed attitude errors related to field of view and pixel noise of the star tracker unit. The error information for the different axes (around/across boresight) of this PES in the sensor frame is taken from the data sheet of the manufacturer. The data sheet provides the errors in the form of parameter values that define a power spectrum for both noise sources.

In general, both noise sources could be realized as single PES (or combined to an overall star tracker noise together with the temporal noise of PES 5). Additionally PEET offers a special block 'Star Tracker Noise' which allows a simple definition of the required parameters which are used to setup the model described below.

3.2.3.2 Model

The PES is described in the PointingSat-SAT-STR reference frame. Therefore all following descriptions of the model are done in that frame.

- **General Parameters:**

The data sheet provides the following parameters for the general parameters (for both cross-axes and boresight axis):

Detector size:	1024 Pixels
Sensor FoV:	30 deg
S/C angular velocity:	360°/d
No. of tracked stars:	N_{stars} = 12
Alpha:	0°
Beta:	90°

Note that the actual number of stars depends mainly on the tracking mode and the on the region of the sky that is being observed. Thus, N_{stars} should be considered as a typical average rather than being a

fixed number. With the parameters above, the PSD of the FOV noise can be modelled using a 1st-order filter as:

$$PSD_{FOV} = \sqrt{\frac{T_{FOV}}{\left|1 + s\frac{T_{FOV}}{2}\right|^2} n_{FOV}^2} \qquad [arcsec/\sqrt{Hz}] \qquad \text{Eq 3-1}$$

The correlation time T_{FOV} is assumed to be proportional to the inverse of the velocity v_{star} (pixels/sec) with which the star image moves on the sensor pixel matrix:

$$T_{FOV} = \frac{1024}{v_{star}\sqrt{N_{stars}}} \ [s] \qquad \text{Eq 3-2}$$

The star velocity itself can be linked to the spacecraft angular velocity ω_{SC} = 360°/day as follows:

$$v_{star} = \omega \frac{1024}{FOV} \sin\beta \cos\alpha \qquad \text{Eq 3-3}$$

where FOV is the sensor field of view in degrees, β is the angle between the sensor boresight and the spacecraft rotation axis and α is the angle between the star image direction of motion on the detector matrix and the reference axis.

The sensor FOV is assumed to be 30° and the sine-cosine product is set to 1 for the sake of simplicity.

The result is a correlation time of T_{FOV} = 2080s.

- **FOV noise:**

The data sheet provides the following parameters for the FOV:

White noise level: n_{FOV} = 0.8 arcsec

- **Pixel noise:**

The data sheet provides the following parameters for the pixel noise on the cross-axes (boresight axis):

Size of centroiding window:	N_{pixels} = 3 (3)
White noise level:	n_{pixel} = 1.5 arcsec (12 arcsec)
Damping of 2nd order filter:	ξ = 0.6 (0.6)

With these parameters, the PSD of the FOV noise can be modelled using a 2nd-order filter as:

$$PSD_{pixel} = \sqrt{\frac{\omega_0^4}{\left|s^2 + 2\xi\omega_0 s + \omega_0^2\right|^2} n_{pixel}^2 T_{pixel}} \quad [arcsec/\sqrt{Hz}] \qquad \text{Eq 3-4}$$

where the characteristic frequency ω_0 is given by:

$$\omega_0 = \frac{4\xi}{T_{pixel}} \qquad \text{Eq 3-5}$$

The correlation time T_{pixel} is again assumed to be proportional to the inverse of the velocity v_{star}:

$$T_{pixel} = \frac{N_{pixels}}{v_{star}} \ [s] \qquad \text{Eq 3-6}$$

with the star velocity computed as for the FOV noise case. The result is a correlation time of T_{pixel} = 21.1s.

The resulting power spectra for both noise sources are illustrated in the figure below:

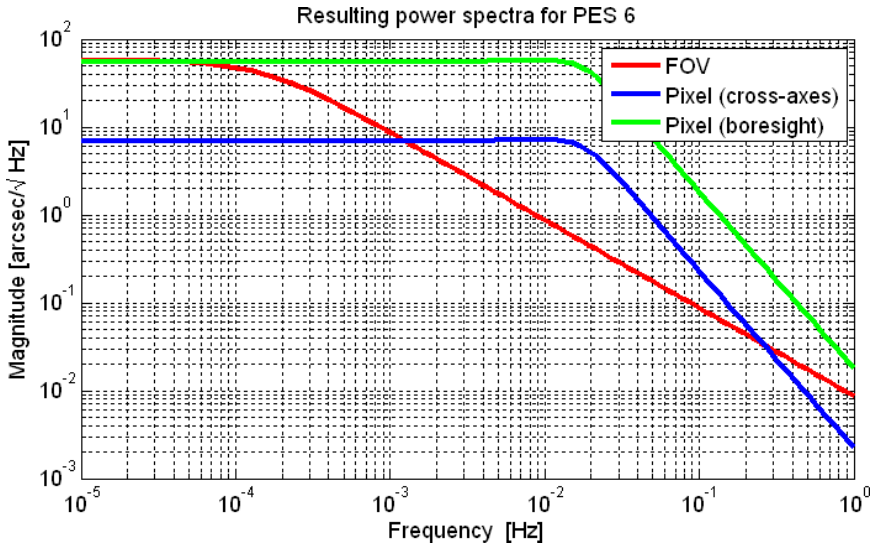

Figure 3-3: FOV and Pixel noise PSDs

- **Total noise:**

Assuming that FOV and pixel noise are uncorrelated, the total PSD for this PES is given by:

PES6 Model	
Type	Random Process
Class	Random
Time-Random	yes
Ensemble-Random	no
Ensemble Domain	Equipment Noise
Physical unit	$[\text{arcsec}/\sqrt{\text{Hz}}]$
Temporal Distribution	Gaussian
Ensemble Distribution	-
Parameter	$\text{PSD}_{6,\text{ax}} = \sqrt{\text{PSD}_{6,\text{ax,pixel}}^2 + \text{PSD}_{6,\text{ax,FOV}}^2}$

Combining above results, PES 6 can be finally expressed as (see also Figure 3-4):

$$\boldsymbol{\alpha}_6 = \begin{bmatrix} PSD_{6,c} \\ PSD_{6,c} \\ PSD_{6,a} \end{bmatrix} \text{arcsec}/\sqrt{\text{Hz}} \qquad \text{Eq 3-7}$$

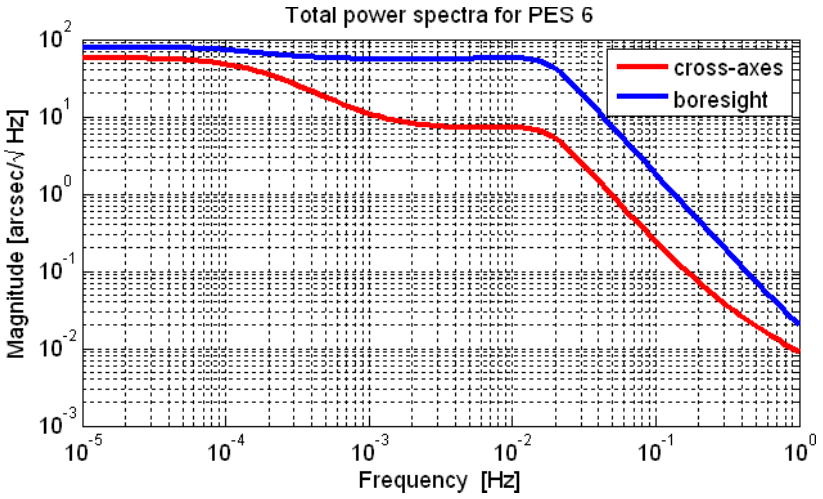

Figure 3-4: Total power spectra for PES6

3.2.4 PES 7: Gyro Noise

3.2.4.1 Description

This PES represents the unprocessed noise on the rate measurements from a gyro assembly (one sensor aligned with each axis, thus the PES can be considered as already converted into the spacecraft body frame).

3.2.4.2 Model

Using typical specifications for a rate sensor, its noise characteristics can be described by:

Angle random walk:	N = 0.0005°/√h
Rate random walk:	K = 0.0001°/h$^{3/2}$
Bias instability:	B = 0.001°/h
Quantization noise:	Q = 3 arcsec
Sample period	T = 0.1s

According to Appendix B in [AD4], this description can be converted into a PSD representation as shown in the Figure below.

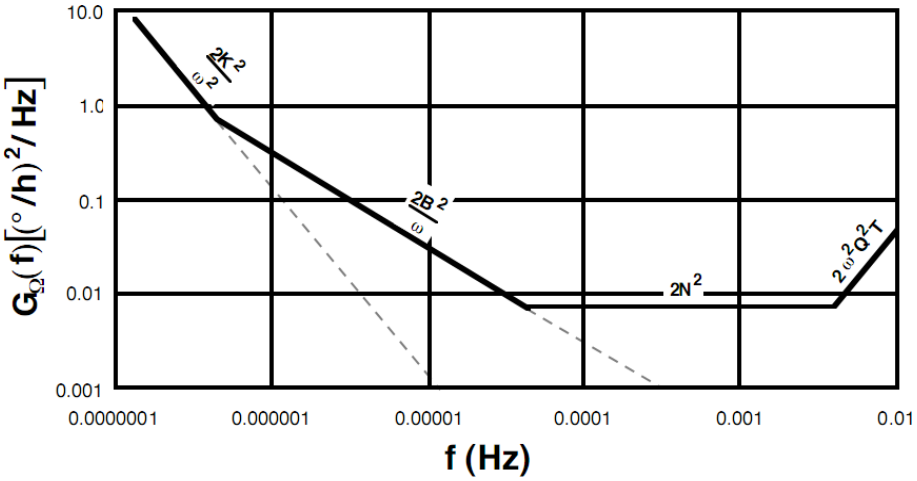

Figure 3-5: Gyro noise PSD derived from typical specifications [AD4]

This PSD could either be defined manually by a set of frequency and magnitude vectors or simply using the special ‘Gyro Rate Noise’ block and providing the above-mentioned parameters. In both cases, PEET performs a rational fit (maximum order 16 in this example) of a transfer function magnitude to the above shape which can be represented by:

PES7 Model	
Type	Random Process
Class	Random
Time-Random	yes
Ensemble-Random	no
Ensemble Domain	Equipment Noise
Physical unit	[arcsec/s]
Temporal Distribution	Gaussian
Ensemble Distribution	-
Parameter	$\mathbf{n}_{\omega,7} = \begin{bmatrix} PSD_{7,x} \\ PSD_{7,y} \\ PSD_{7,z} \end{bmatrix}$

where $PSD_{7,ax}$ describes the rate noise on the respective axis ax (identical in this case for all axes). For the parameters above, the resulting PSD is shown in Figure 3-6.

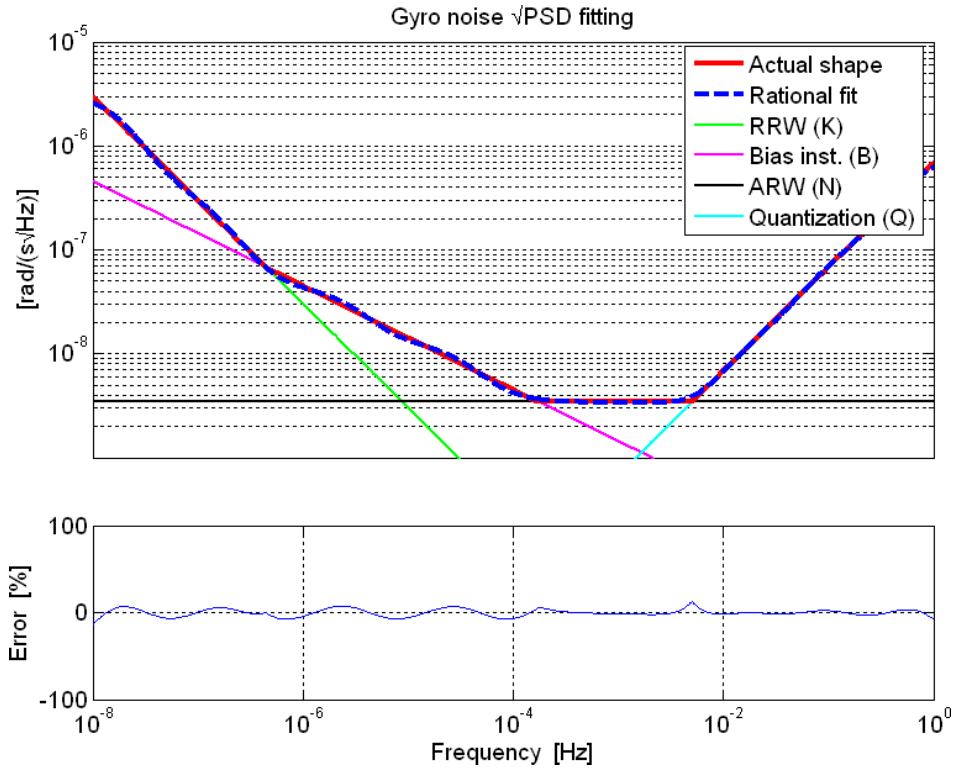

Figure 3-6: Gyro noise PSD for given parameters

3.2.5 PES 8: Cryocooler Micro-Vibrations

3.2.5.1 Description

This PES represents the impact of micro-vibrations induced by the cryogenic cooling device on the pointing error.

3.2.5.2 Model

As micro-vibrations are dominated by periodic components, the PES can be modelled as RP type Periodic which is defined by frequency and amplitude. From measurements, the amplitudes of the micro-vibration force at a fundamental frequency f_8 = 57.5 Hz and higher harmonics is given (see Figure 3-7). With these discrete values, the PES can be modelled as:

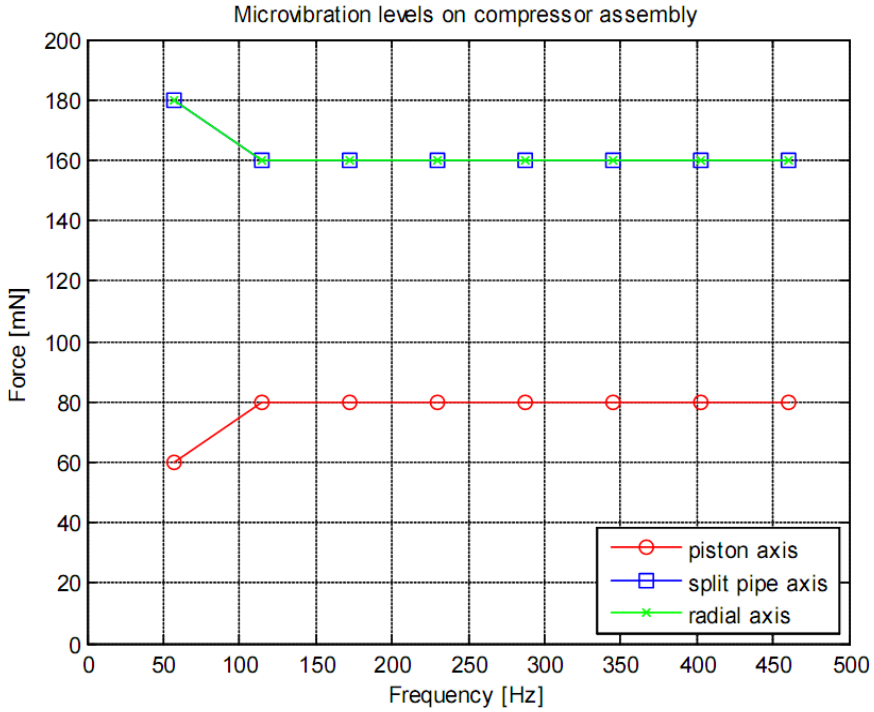

Figure 3-7: Cryocooler micro-vibration levels at distinct frequencies

PES8 Model	
Type	Random Variable
Class	Periodic
Time-Random	yes
Ensemble-Random	no
Ensemble Domain	Equipment Noise
Physical unit	$[\mathrm{mN}]$
Temporal Distribution	Bimodal
Ensemble Distribution	Uniform
Parameter	$\boldsymbol{\alpha}_8 = \begin{bmatrix} P\left(\mathbf{f}_8, U\left(\mathbf{A}_{8,x,\min}, \mathbf{A}_{8,x,\max}\right)\right) \\ P\left(\mathbf{f}_8, U\left(\mathbf{A}_{8,y,\min}, \mathbf{A}_{8,y,\max}\right)\right) \\ P\left(\mathbf{f}_8, U\left(\mathbf{A}_{8,z\min}, \mathbf{A}_{8,z,\max}\right)\right) \end{bmatrix} = \begin{bmatrix} P([57.5;115],[175,185;155,165]) \\ P([57.5;115],[175,185;155,165]) \\ P([57.5;115],[55,65;75,85]) \end{bmatrix}$

where $\mathbf{f}_8$ depicts a vector consisting of the fundamental frequency f_8 and the considered harmonics (i.e. multiples of f_8). $\mathbf{A}_{8,ax}$ represents the vector of the respective amplitudes for each axis ax. For the sake of simplicity, only the first two harmonics will be considered for the PointingSat example. The amplitude of the micro-vibrations have due to different operational conditions a Uniform ensemble distribution.

3.3 Ensemble-Domain 3: External Environment

All effects from the external environment are summarized in the 'External Environment' ensemble domain. This covers the environmental disturbance torques on the satellite and all thermal effects. As the origin of these PES is not internal of the satellite system, they can be arranged in the same ensemble domain for an equal evaluation.

PES 9 to PES 11 represent the same error source, namely external environmental disturbance torques. In case of PointingSat, the solar radiation pressure is identified as the driving disturbance source with only minor influence of the gravity gradient and magnetic field torques.

Simulations using worst case model settings for the satellite environment and a simplified satellite surface model have been performed for PointingSat. Data are available as time-series from these simulations which were be pre-processed such that they can be used within PEET.

First, the ensemble distribution of the biases is identified as one PES. Furthermore a linear trend is translated to a drift error with a reset time set to infinity. From the residual noise part a PSD is estimated. Although PEET does provide an auxiliary, basic function to automatically generate a PSD from a time-series, such data processing is generally up to the user as different estimation techniques and different window functions can be used to address different aspects of the signal.

3.3.1 PES 9: Environmental Disturbances Constant Part

3.3.1.1 Description

This PES represents the torque biases of the environmental disturbance.

3.3.1.2 Model

PES9 Model	
Type	Random Variable
Class	Bias
Time-Random	no
Ensemble-Random	yes
Ensemble Domain	External Environment
Physical unit	$[\,\mathrm{mNm}\,]$
Temporal Distribution	Discrete
Ensemble Distribution	Gaussian
Parameter	$\mathbf{B}_9 = \begin{bmatrix} \delta\left(G\left(\mu_{9,x},\sigma_{9,x}\right)\right) \\ \delta\left(G\left(\mu_{9,y},\sigma_{9,x}\right)\right) \\ \delta\left(G\left(\mu_{9,z},\sigma_{9,z}\right)\right) \end{bmatrix} = \begin{bmatrix} \delta\left(G\left(1.0,0.5\right)\right) \\ \delta\left(G\left(2.0,0.5\right)\right) \\ \delta\left(G\left(0.8,0.5\right)\right) \end{bmatrix}$

The bias derived from each axis of the environmental disturbance is a time constant for each realization which is covered by a CRV type PES. The ensemble variation is represented by a Gaussian distribution.

3.3.2 PES 10: Environmental Disturbances Drift Part

3.3.2.1 Description

This PES describes the linear trend of the environmental disturbances as described for PES9.

3.3.2.2 Model

The PES is modelled as a drift type using the slope D of the trend and as reset time the overall time span of the time series.

PES10 Model	
Type	Random Variable
Class	Drift
Time-Random	yes
Ensemble-Random	yes
Ensemble Domain	External Environment
Physical unit	$[\,Nm\,]$
Temporal Distribution	Uniform (Drift)
Ensemble Distribution	Gaussian
Parameter	$\boldsymbol{\varepsilon}_{D,10} = \begin{bmatrix} \varepsilon_D\left(G\left(0,\sigma_{10,x}\right),\Delta t_{10,D}\right) \\ \varepsilon_D\left(G\left(0,\sigma_{10,y}\right),\Delta t_{10,D}\right) \\ \varepsilon_D\left(G\left(0,\sigma_{10,z}\right),\Delta t_{10,D}\right) \end{bmatrix} = \begin{bmatrix} \varepsilon_D\left(G\left(0,-1.00\cdot10^{-16}\right),10^6\right) \\ \varepsilon_D\left(G\left(0,-1.56\cdot10^{-16}\right),10^6\right) \\ \varepsilon_D\left(G\left(0,-8.04\cdot10^{-17}\right),10^6\right) \end{bmatrix}$

where $\sigma_{10,ax}$ describes the standard deviation of the drift rate for axis ax and $\Delta t_{10,D}$ the overall time span of the time series.

Note that $\Delta t_{10,D}$ should be much larger than the window time and stability time for the RPE and PRE indices to properly describe the drift.

Due to variations of the environmental disturbances over a large time scale, the drift rate $D_{10,ax}$ is assumed to be Gaussian distributed over the ensemble of possible realizations.

3.3.3 PES 11: Environmental Disturbances Noise Part

3.3.3.1 Description

This PES describes the remaining part of the environmental disturbances as described for PES9 and PES10.

3.3.3.2 Model

The remaining part after bias removal and detrending is described as an RP type PES in terms of PSD, i.e.

PES11 Model	
Type	Random Process
Class	Random
Time-Random	yes
Ensemble-Random	no
Ensemble Domain	External Environment
Physical unit	$[\,\mathrm{Nm}/\sqrt{\mathrm{Hz}}\,]$
Temporal Distribution	Gaussian
Ensemble Distribution	-
Parameter	$\mathbf{n}_{Trq,11} = \frac{1\cdot 10^{-9}}{s+0.01}\begin{bmatrix}1.2\\2.85\\0.95\end{bmatrix}$

where $PSD_{11,ax\text{-}ax}$ describes the noise auto power spectral density on axis ax. Figure 3-8 depicts the PSD from the environmental disturbance simulation. A fitting PSD is chosen for each axis as simplification.

Note: The PSD from the simulation has also cross power spectra, which are not represented in Figure 3-8.

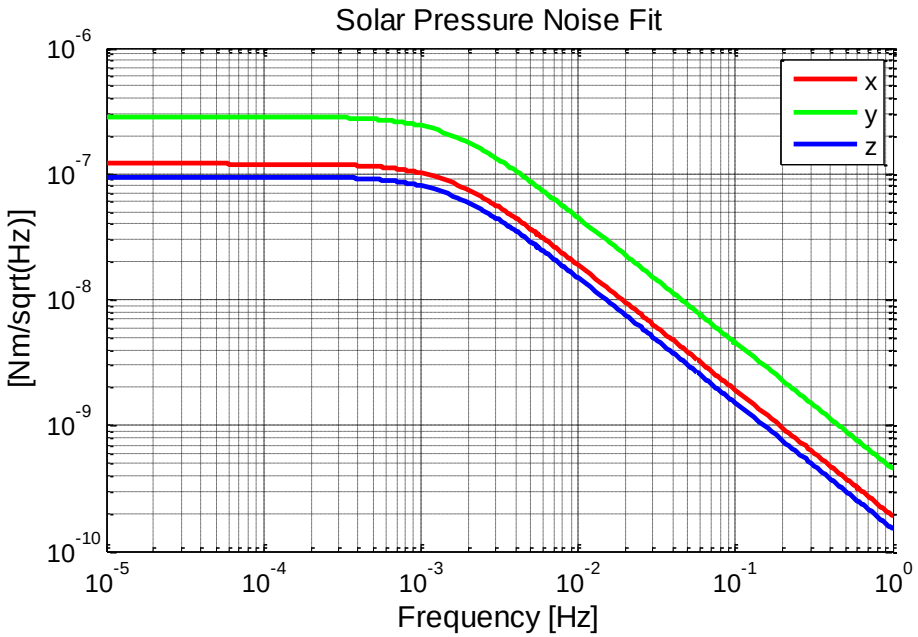

Figure 3-8Solar pressure torque noise (PSD and fit)

3.3.4 PES 12: Thermo-Elastic Distortion: Payload – Star Tracker Mounting Plate (Periodic Part)

3.3.4.1 Description

This PES represents periodic part at orbital frequency (1/day) of thermo-elastic distortion between the payload and the mounting plate of the star tracker. The amplitude of this periodic error is assumed to be dependent on the DC operational temperature.

3.3.4.2 Model

As the PES describes a periodic signal, it can be modelled as PES of type Periodic. This type is defined by its frequency and the distribution of the amplitude. Assuming a linear dependence on the DC temperature which is required to be within a defined operation range only, the amplitude of the PES can be modelled with a uniform distribution, i.e.

PES12 Model	
Type	Random Process
Class	Random
Time-Random	yes
Ensemble-Random	no
Ensemble Domain	External Environment
Physical unit	[arcsec]
Temporal Distribution	Bimodal
Ensemble Distribution	Uniform
Parameter	$\boldsymbol{\alpha}_{12} = \begin{bmatrix} P(f_{12}, U(A_{12,\min,x}, A_{12,\max,x})) \\ P(f_{12}, U(A_{12,\min,y}, A_{12,\max,y})) \\ P(f_{12}, U(A_{12,\min,z}, A_{12,\max,z})) \end{bmatrix} = \begin{bmatrix} P(f_{12}, U(5,15) \\ P(f_{12}, U(4,10) \\ P(f_{12}, U(1,5) \end{bmatrix}$ $f_{12} = \frac{1}{day}$

where $A_{12,min,ax}$ ($A_{12,max,ax}$) describes the distortion amplitude for the respective axis ax (related to the minimum (maximum) permitted operational DC temperature).

3.3.5 PES 13: Thermo-Elastic Distortion: Payload – Star Tracker Mounting Plate (Transient Part)

3.3.5.1 Description

This PES represents the thermo-elastic transient behaviour due to eclipse phases during spring and autumn equinoxes.

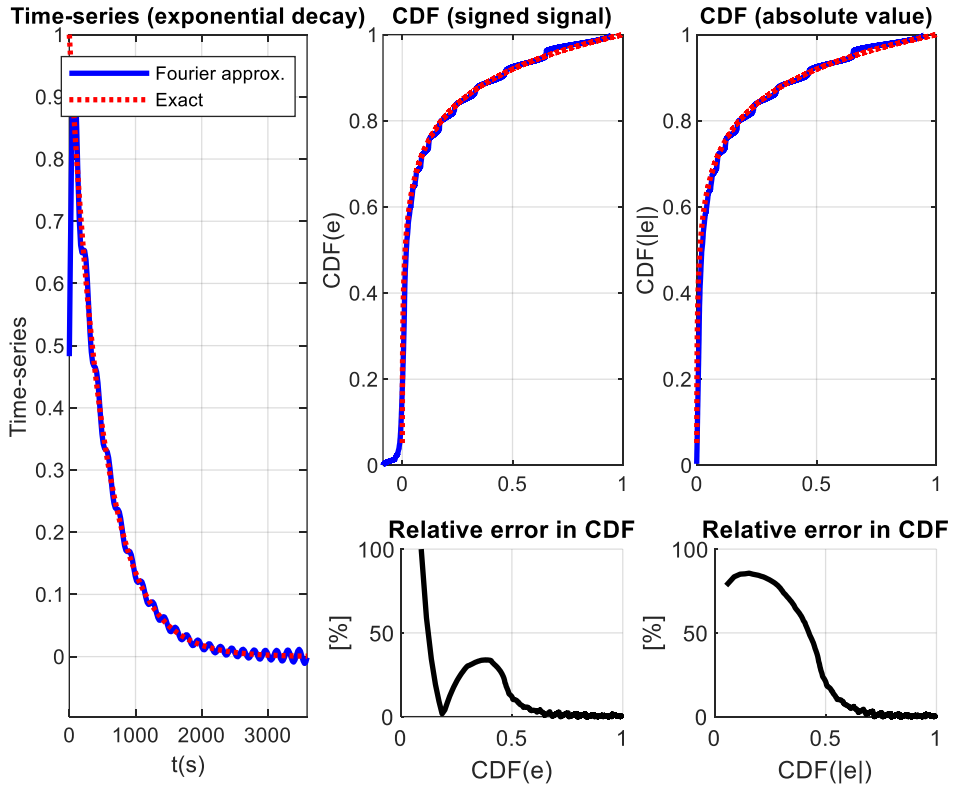

Figure 3-9: Transient effects in thermos-elastic distortions between payload and STR mounting plate during eclipse phases at spring and autumn equinoxes

3.3.5.2 Model

Assume that - given the characteristics from the datasheet - the PES can be modelled as:

PES13 Model	
Type	Transient (General Periodic Signal)
Class	Exponential Decay
Time-Random	no
Ensemble-Random	no
Ensemble Domain	External Environment
Physical unit	[arcsec]
Temporal Distribution	
Ensemble Distribution	-
Parameter	Fundamental period 4320 s Decay rate: 0.002 Amplitude: [6.0 4.0 2.0] arcsec

3.3.6 PES 14: Thermo-Elastic Distortion: Payload – Star Tracker Mounting Plate (Random Part)

3.3.6.1 Description

This PES represents the random/noise part of the thermo-elastic distortion between the payload and mounting plate of the star tracker. There is no exact model available for this effect, only a linear dependence on the operational DC temperature is expected.

3.3.6.2 Model

According to these presetting, the random part can be modelled as a RV type PES with zero mean and Gaussian distribution. The variance of the PES is not constant, but uniformly distributed between upper and lower bounds related to effective DC operational temperature.

PES14 Model	
Type	Random Variable
Class	Random
Time-Random	yes
Ensemble-Random	yes
Ensemble Domain	External Environment
Physical unit	[arcsec]
Temporal Distribution	Gaussian
Ensemble Distribution	Uniform
Parameter	$\boldsymbol{\alpha}_{13} = \begin{bmatrix} G(0, U(\sigma_{13,\min,x}, \sigma_{13,\max,x})) \\ G(0, U(\sigma_{13,\min,y}, \sigma_{13,\max,y})) \\ G(0, U(\sigma_{13,\min,z}, \sigma_{13,\max,z})) \end{bmatrix} = \begin{bmatrix} G(0, U(1,2)) \\ G(0, U(1,2)) \\ G(0, U(1,2)) \end{bmatrix}$

where $\sigma_{13,min,ax}$ and $\sigma_{13,max,ax}$ describe the standard deviation on the axis ax related to the minimum and maximum DC operational temperature range.

3.3.7 PES 15: Star Tracker Internal Thermal Distortions

3.3.7.1 Description

The PES describes the thermos-elastic distortions at orbital frequency (1/day), which affect the alignment of the star tracker mounting plate to the internal axes of the star tracker. The amplitude of this periodic error is assumed to be dependent on the DC operational temperature.

3.3.7.2 Model

As the PES describes a periodic signal, it can be modelled as PES of type Periodic. As it describes the same error source as PES 12 between different parts of the satellite, it can be modelled in an equal form with a uniform ensemble distribution of the amplitude, i.e.

PES15 Model	
Type	Random Variable
Class	Periodic
Time-Random	yes
Ensemble-Random	yes
Ensemble Domain	External Environment
Physical unit	[arcsec]
Temporal Distribution	Bimodal
Ensemble Distribution	Uniform
Parameter	$\boldsymbol{\alpha}_{14} = \begin{bmatrix} P(f_{14}, U(A_{14,\min,x}, A_{14,\max,x})) \\ P(f_{14}, U(A_{14,\min,y}, A_{14,\max,y})) \\ P(f_{14}, U(A_{14,\min,z}, A_{14,\max,z})) \end{bmatrix} = \begin{bmatrix} P(f_{14}, U(2,4) \\ P(f_{14}, U(4,7) \\ P(f_{14}, U(0.5,2) \end{bmatrix}$ $f_{14} = \frac{1}{day}$

3.3.8 PES 16: Thermal Stability Effect on Star Tracker

3.3.8.1 Description

This PES represents a temperature dependent part of the noise in the star tracker measurement, e.g. thermal distortions of the detector pixel array. From analysis, only the temperature stability at one reference point on the optical bench is known and the transfer behaviour from this reference to star tracker detector has been estimated.

3.3.8.2 Model

The PES is described in the PointingSat-SAT-STR reference frame. Therefore all following descriptions of the PES are done in this frame.

The temperature stability at the reference point is given in terms of a power spectrum leading to a PES model of the form:

$$\mathbf{n}_{T,15} = PSD_{15} \quad [\,\mathrm{K}/\sqrt{\mathrm{Hz}}\,] \qquad \text{Eq 3-8}$$

Note that the described temperature stability is 'one-dimensional', i.e. it cannot be assigned to a physical pointing axis at this point. Proper mapping to physical axis is then realized in the system transfer models. The model used to describe the temperature stability at the measured reference points is given in Figure 3-10.

To highlight the different options for PES definition in PEET, PES 16 is set up as a state-space model equivalent to the transfer function given above:

PES16 Model	
Type	Random Process
Class	Random
Time-Random	yes
Ensemble-Random	no
Ensemble Domain	External Environment
Physical unit	$[\,\mathrm{K}/\sqrt{\mathrm{Hz}}\,]$
Temporal Distribution	Gaussian
Ensemble Distribution	-
Parameter	State-space representation of PSD with $A=-0.008\begin{bmatrix}1&0&0\\0&1&0\\0&0&1\end{bmatrix}; B=0.25\begin{bmatrix}1&0&0\\0&1&0\\0&0&1\end{bmatrix};$ $C=0.3584\begin{bmatrix}1&0&0\\0&1&0\\0&0&1\end{bmatrix}; D=\begin{bmatrix}0&0&0\\0&0&0\\0&0&0\end{bmatrix}$

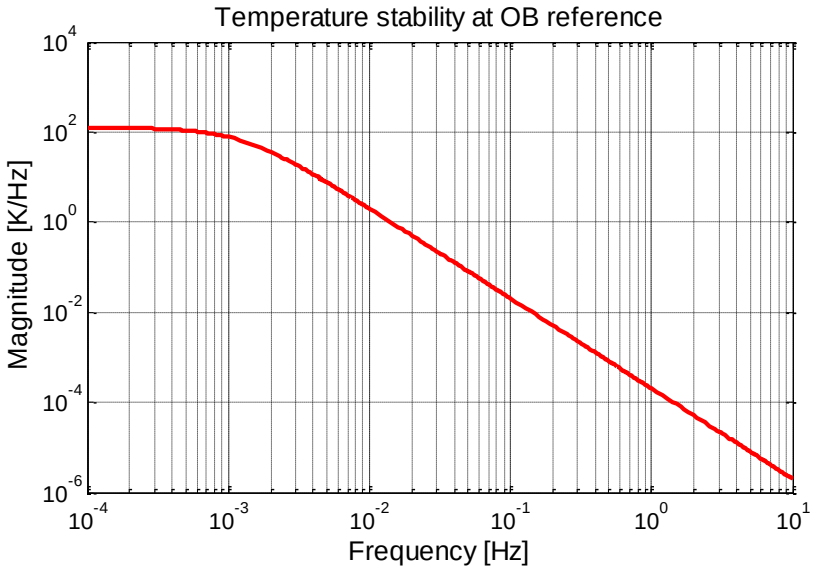

Figure 3-10: Thermal stability at optical bench reference point

3.3.9 PES 17: Thermal Stability Effect on Payload

3.3.9.1 Description

This PES represents a temperature stability induced noise that affects the position of the focal point of the telescope and in consequence directly the pointing. From analysis - as in case of PES 16 - only the temperature stability at one reference point on the optical bench is known and the transfer behaviour to from this reference to the focal point location has been estimated.

3.3.9.2 Model

The temperature stability at the reference point is given in terms of a power spectrum leading to a PES model of the form:

$$n_{T,16} = n_{T,16} = PSD_{16}\ [\mathrm{K}/\sqrt{\mathrm{Hz}}] \qquad \text{Eq 3-9}$$

Again, a different representation in terms of a zpk-model is used for PES16 which is equivalent to the state-space definition of PES 15.

PES17 Model	
Type	Random Process
Class	Random
Time-Random	yes
Ensemble-Random	no
Ensemble Domain	External Environment
Physical unit	$[\mathrm{K}/\sqrt{\mathrm{Hz}}]$
Temporal Distribution	Gaussian
Ensemble Distribution	-
Parameter	Zero-Pole-Gain representation with $z = [\,] \quad p = -0.008 \quad k = 0.0896$

3.4 Ensemble Domain 4: Station Keeping Manoeuvre

All effects related to station keeping manoeuvres (SKM) are summarized in the ‘Station Keeping Manoeuvre’ ensemble domain.

3.4.1 PES 18: Station Keeping Manoeuvre Control Performance Error Transient

3.4.1.1 Description

This PES represents the transients in the pointing control performance error after a station keeping manoeuvre, which are caused by the decaying oscillation of the solar arrays after the Delta-V impuls.

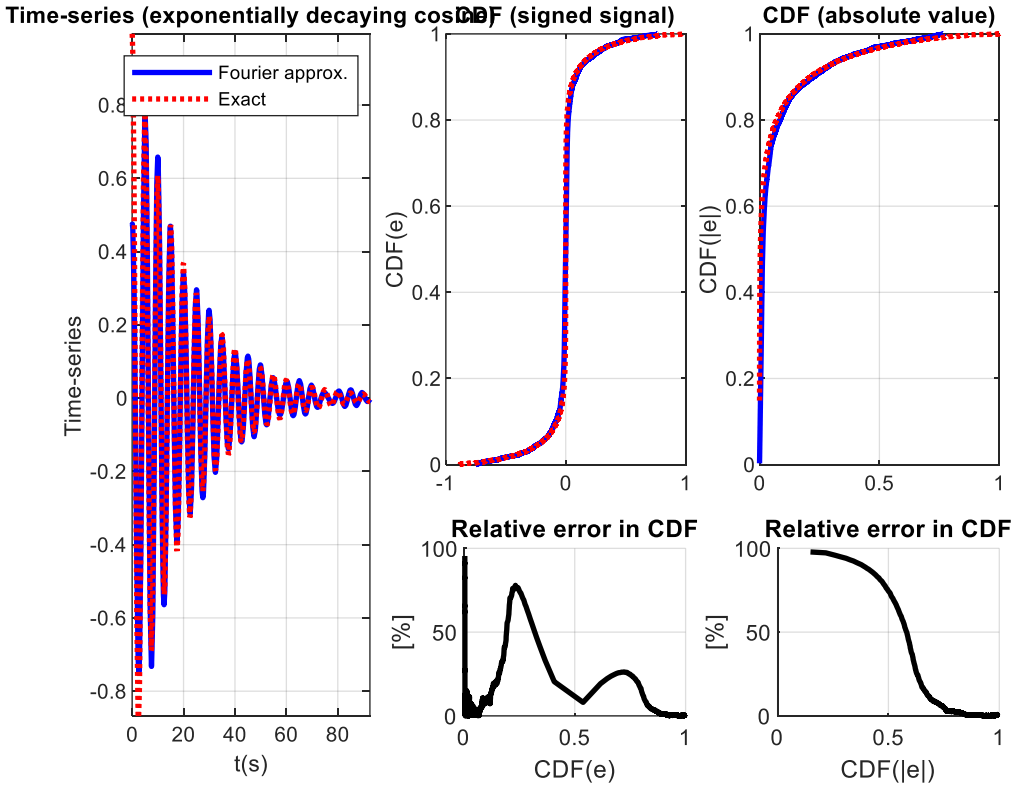

Figure 3-11: Transient effects in pointing control performance error after station keeping manoeuvre

Note that the fundamental period should be longer here. However this would require a higher order of the Fourier approximation to provide a good fit.

3.4.1.2 Model

Assume that - given the characteristics from the datasheet - the PES can be modelled as:

PES18 Model	
Type	Transient (General Periodic Signal)
Class	Decaying Cosine
Time-Random	no
Ensemble-Random	no
Ensemble Domain	Station Keeping Manoeuvre
Physical unit	[deg]
Temporal Distribution	
Ensemble Distribution	-
Parameter	Fundamental period 200 s Decay rate: 0.05 Cosine frequency: 0.2 Hz Amplitude: [0.012 0.01 0.011] deg

3.5 PES Summary

The following table summarizes the types and description for the different PES of PointingSat.

Table 3-1: PES Summary

PES No.	Type	Description
1	CRV	Mechanical alignment between payload and star tracker
2	CRV	Misalignment between payload and star tracker due to launch effects
3	CRV	Star tracker measurement bias
4	Transient	Reaction wheel steps and spikes
5	RP (Covariance)	Star tracker temporal measurement noise (temperature/orientation independent part)
6	RP (PSD)	Star tracker FOV and pixel noise
7	RP (PSD)	Rate noise of gyro assembly
8	RP (Periodic)	Cryocooler induced micro-vibrations
9	CRV	Constant environmental disturbances on satellite body
10	Drift	Drift environmental disturbances on satellite body
11	RP(PSD)	Noise environmental disturbances on satellite body
12	RP (Periodic)	Periodic part of thermo-elastic distortion affecting the alignment between payload to

		star tracker mounting plate
13	Transient	Transient part of thermo-elastic distortion affecting the alignment between payload to star tracker mounting plate
14	RV	thermo-elastic distortion affecting the alignment between payload to star tracker mounting plate
15	RP (Periodic)	Thermo-elastic distortion affecting the alignment of the internal star tracker axes to the mounting plate
16	RP (PSD)	Thermal stability effect on star tracker measurement
17	RP (PSD)	Thermal stability effect on focal point stability
18	Transient	Transient effects in pointing control performance error after station keeping manoeuvre

3.6 Correlation

According to [AD1], assumptions on the correlation between different PES are required to perform the final pointing error evaluation. In PEET, correlation is defined in the global settings.

The 'evolution' of the correlation through the system transfer (e.g. cross-coupling of axes, addition of signals, etc.) is automatically tracked by the software. The following chapters summarize the initial correlation state of the different PES determined by measurements in the system identification process.

3.6.1 Ensemble-Domain 1: Assembly and Launch

3.6.1.1 Time Parameter

- **Correlation between random variable described PES:**

Table 3-2: Correlation between random variable described PES of Ensemble-Domain 1

	PES 1	**PES 2**	**PES 3**
PES 1	1	0	0
PES 2	0	1	0
PES 3	0	0	1

Between the different PES of the ensemble-domain 1 there is no temporal correlation. This arises as all random variable described PES in this domain are constant over time and therefore they do by definition not correlate.

3.6.1.2 Ensemble Parameter

Table 3-3: Axis correlation setting of Ensemble-Domain 1

	PES 1x	**PES 1y**	**PES 1z**
PES 1x	1	1	1
PES 1y	1	1	1
PES 1z	1	1	1

PES 1 (Mechanical Payload to Star Tracker Alignment): As the alignment measurement for the payload telescope and the star tracker is based on theodolite measurements, it is conceivable that the knowledge errors of three axes are not independent from each other. For that reason, knowledge errors of the PES are assumed to be fully correlated among the different axes.

Table 3-4: Ensemble Parameter Correlation of Ensemble-Domain 1

	PES 1	**PES 2**	**PES 3**
PES 1	1	0.3	0
PES 2	0.3	1	0
PES 3	0	0	1

The launch changes the alignment between STR and Payload. Hence, the ensemble parameter of PES 1 (Mechanical Payload to Star Tracker Alignment) and PES 2 (Star Tracker to Payload Alignment after Launch) approach closer to each other. This leads to the specified ensemble parameter correlation coefficient.

PES 3 (Star Tracker Bias) is assumed to be fully uncorrelated with all other PES as they have no 'physical' link to other PES.

3.6.2 Ensemble-Domain 2: Equipment Noise

3.6.2.1 Time Parameter

- **Coherence between random process described PES**

Table 3-5: Coherence between random process described PES of Ensemble-Domain 2

	PES 4	PES 5	PES 6	PES7
PES 4	1	0	0	0
PES 5	0	1	0	0
PES 6	0	0	1	0
PES 7	0	0	0	1

As PES 4 (RW torque error) consists of only one component and is not described in the three dimensional space. That means that no correlation between axes can be specified.

PES 5 (Star Tracker Noise (Temporal)): As no information about the axes cross-coupling is available, the off-diagonal terms of the covariance matrix are zero, i.e. no correlation between PES 5 axes.

PES 6 (Star Tracker FOV and Pixel Spatial Errors): As no information about the axes cross-coupling is available, the off-diagonal terms of the spectral density matrix are zero, i.e. no correlation between PES 6 axes.

PES 7 (Gyro Noise): Although the information of the body rate is obtained from identical sensors in the gyro assembly, no correlation between the different axes of PES 7 is assumed (as each of the sensors is aligned with the one of the body axis and no 'mixing' of measurement from different gyros is required to obtain a single body axis rate component).

Between the different RP described PES within this ensemble-domain there is no information available for describing a coherence. Therefor the coherence matrix is set to an identity matrix.

- **Phase setting for periodic described PES**

Table 3-6: Phase setting for periodic described PES of Ensemble-Domain 2

	PES 8x	PES 8y	PES 8z
PES 8x	0	0	0
PES 8y	0	0	0
PES 8z	0	0	0

PES 8 (Cryocooler Micro-Vibrations): As the vibration loads affect all spatial directions of the spacecraft structure simultaneously, the different axes of PES 8 are assumed to be fully correlated.

Note: Setting the relative phase between two error sources to zero correlates the PES fully.

3.6.2.2 Ensemble Parameter

Table 3-7: Ensemble Parameter Correlation of Ensemble-Domain 2

	PES 4	PES 5	PES 6	PES7	PES8
PES 4	1	0	0	0	0
PES 5	0	1	0	0	0
PES 6	0	0	1	0	0
PES 7	0	0	0	1	0
PES8	0	0	0	0	1

PES 4 (RW steps and spikes) is assumed to be uncorrelated with other PES as they have no 'physical commonalities'. Note, that due to the mapping of a 1D source to a 3D error according to the mapping matrix for the pyramid configuration of five RWs, the errors in all five RWs are fully correlated. This corresponds to the worst-case of steps and spikes occurring at all five RWs at the same time.

PES 5 (Star Tracker Noise (Temporal)): Due to the sensor intrinsic properties of the noise, there is no correlation with other PES as well.

PES 6 (Star Tracker FOV and Pixel Spatial Errors): Due to the sensor intrinsic properties of the noise, there is no correlation with other PES as well.

PES 7 (Gyro Noise): The noise of the gyro arises independent of any other PES and is therefore assumed to be fully uncorrelated with other PES.

PES 8 (Cryocooler Micro-Vibrations): Micro-vibrations have no direct physical dependence to any of the other described PES in this ensemble-domain. Therefore there is no correlation between PES 8 and any other PES.

3.6.3 Ensemble-Domain 3: External Environment

3.6.3.1 Time Parameter

- **Correlation between random variables described PES**

PES 9 (Environmental Disturbances (Constant Part)): Equally to PES1 to PES3 a time-constant random variable has by definition a temporal correlation of zero.

PES 10 (Environmental Disturbances (Drift Part)): This error source is described by a drift signal. Correlation can only be depicted between different drift signals. The correlation between the different axes is indirectly set by an equal reset time of the signal and the drift slope.

Table 3-8: Correlation setting for random variable described PES of Ensemble-Domain 3

	PES 14x	PES 14y	PES 14z
PES 14x	1	1	1
PES 14y	1	1	1
PES 14z	1	1	1

PES 14 (Thermo-Elastic Distortion (Random Part)): As the thermal distortion affects all spatial directions of the spacecraft structure at the same time in the same way (assuming an isotropic thermal expansion coefficient for the relevant structures), the different axes of PES 14 are assumed to be fully correlated.

- **Coherence between random process described PES**

Table 3-9: Coherence setting for random process described PES of Ensemble-Domain 3

	PES 11	PES 16	PES 17
PES 11	1	0	0
PES 16	0	1	1
PES 17	0	1	1

PES11 (Environmental Disturbances (Noise Part)): The axis correlation is defined by the definition of PSDs on the non-diagonal entries. In this PES the non-diagonal PSD are given by the simulation for the environmental disturbances. Hence, no coherence has to be defined. Furthermore there is no coherence between PES11 and the remaining random process described PES of this ensemble-domain due to unavailable information.

PES 16 and PES 17 (Thermal Stability Effect on Star Tracker and Payload): Although there is only one non-zero component in each of the two PES, the correlation state between its axis is arbitrary and therefore defined as an identity matrix in this study. However, PES 15 is fully correlated with PES 16, as they basically represent the same source.

- **Phase setting for periodic described PES**

Table 3-10: Phase setting for periodic described PES of Ensemble-Domain 3

	PES 12	PES 15
PES 12	0	0
PES 15	0	0

PES 12 (Thermo-Elastic Distortion (Periodic Part)): As the thermal distortion affects all spatial directions of the spacecraft structure at the same time in the same way (assuming an isotropic thermal expansion coefficient for the relevant structures), the different axes of PES 12 are assumed to be fully correlated. Therefore the relative phase is set to zero.

PES 15 (STR Internal Thermo-Elastic Distortion): As PES 12 and PES 15 arise from the same physical phenomenon they basically represent the same error source on different parts of the satellite. Therefore

they are fully correlated with each other. Furthermore due to the same reason as mentioned in PES12 the axes are assumed to be fully correlated. Therefore the relative phase is set to zero and due to unavailable information the relative phase between PES12 and PES15 is set to zero as a worst-case assumption.

3.6.3.2 Ensemble Parameter

Table 3-11: Ensemble Parameter Correlation of Ensemble-Domain 3

	PES 9	PES 10	PES 11	PES 12	PES 13	PES 14	PES 15	PES 16	PES 17
PES 9	1	1	1	0	0	0	0	0	0
PES 10	1	1	1	0	0	0	0	0	0
PES 11	1	1	1	0	0	0	0	0	0
PES 12	0	0	0	1	0	0	1	0	0
PES 13	0	0	0	0	1	0	0	0	0
PES 14	0	0	0	0	0	1	0	0	0
PES 15	0	0	0	1	0	0	1	0	0
PES 16	0	0	0	0	0	0	0	1	1
PES 17	0	0	0	0	0	0	0	1	1

PES 9 – PES 11 (Environmental Disturbances): No correlation between these PES and any other PES is assumed. Between PES 9 – PES 11 there is full correlation assumed in the ensemble-parameter, as they represent the different aspects of one physical phenomenon.

PES 12 (Thermo-Elastic Distortion (Periodic Part)): PES 12 and PES 15 represent the same error source on different parts of the satellite. In the ensemble they are both dependent on the DC operational temperature. Therefore they are due to missing detailed information assumed to be fully correlated with each other.

PES 14 (Thermo-Elastic Distortion (Random Part)): There is no correlation between PES 14 and any other PES assumed.

PES 15 (STR Internal Thermo-Elastic Distortion): PES 15 is fully correlated with PES 12 as stated for its description.

PES 16 and PES 17 (Thermal Stability Effect on Star Tracker and Payload): Although there is only one non-zero component in the PES, the correlation state between its axis is arbitrary. However, PES 16 is fully correlated with PES 17, as they basically represent the same source.

3.6.4 Ensemble-Domain 4: Station Keeping Manoeuvre

3.6.4.1 Time Parameter

- **Phase setting for periodic described PES**

Table 3-12: Phase setting for periodic described PES of Ensemble-Domain 4

	PES 18
PES 18	0

3.6.4.2 Ensemble Parameter

Table 3-13: Ensemble Parameter Correlation of Ensemble-Domain 3

	PES 18
PES 18	0

4 Transfer Analysis (AST-2)

This section covers the transfer analysis of the PES according to AST-2 in [AD1]. The first subsection describes the system transfer for each PES in general, the second subsection defines the applied system models.

4.1 PES System Transfers

4.1.1 PES 1: Mechanical Payload and Star Tracker Alignment

As the measurement error knowledge is provided with respect to the satellite body axes (coinciding with the nominal payload axes), no further system transfer is required, i.e. PES 1 directly represents a PEC.

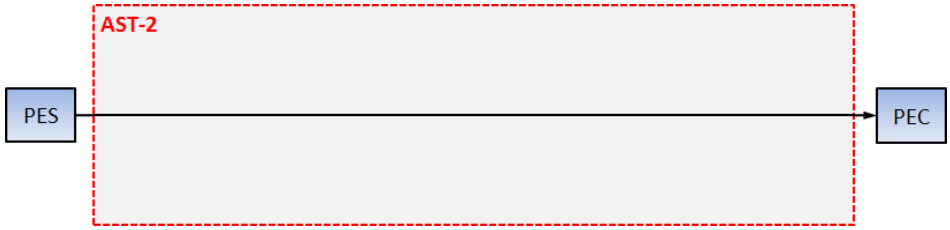

Figure 4-1: System transfer of PES 1 (according to AST-2 in [AD1])

4.1.2 PES 2: Star Tracker to Payload Alignment after Launch

As the payload to star tracker misalignment directly describes relevant error information, no further system transfer is required, i.e. PES 2 directly represents a PEC.

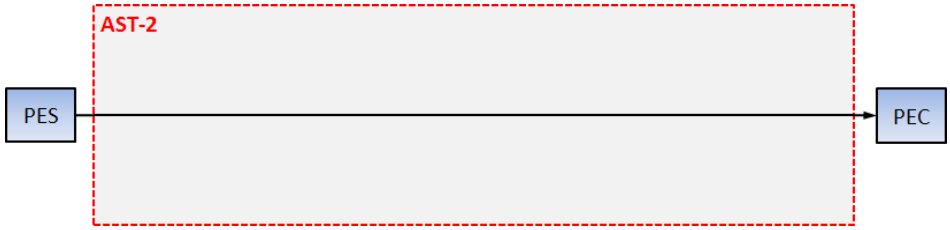

Figure 4-2: System transfer of PES 2 (according to AST-2 in [AD1])

4.1.3 PES 3: Star Tracker Bias

As the nominal sensor (more precisely the camera head) frame has a different orientation compared to the satellite body axes, PES 3 first has to be fed through a Coordinate Transformation (CTF), the Gyro-Stellar Estimator (GSE) and the Feedback system in order to represent a PEC in the correct frame.

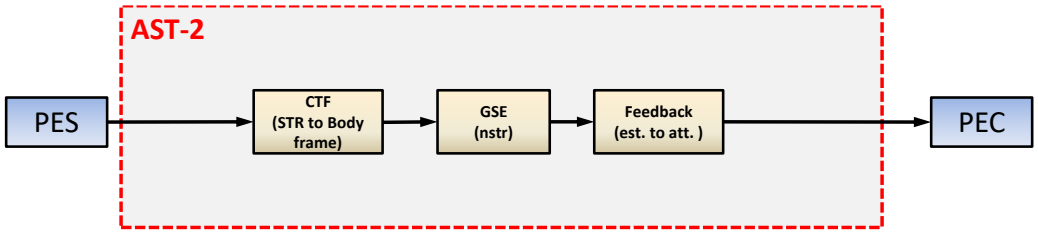

Figure 4-3: System transfer of PES 3 (according to AST-2 in [AD1])

4.1.4 PES 4: Reaction Wheel Steps and Spikes

As PES 4 only represents one single actuator of the whole assembly, the torque error of one individual RW has to be converted to a torque noise from the entity of RWs first. This is done via the actuation matrix describing the orientation and position of all actuators in the body frame. The resulting torque noise is then treated as disturbance input η_d on the satellite plant in the closed-loop feedback system. It is thus turned into a PEC by applying the closed-loop transfer function matrix from disturbance input η_d to the control variable y (representing the pointing angles).

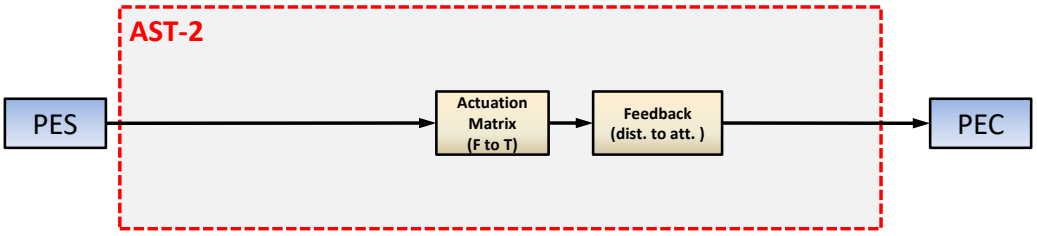

Figure 4-4: System transfer of PES 4 (according to AST-2 in [AD1])

4.1.5 PES 5: Star Tracker Noise (Temporal)

The PES itself describes one part of the unprocessed measurement noise of the star tracker in its sensor frame. Thus, it first has to be expressed in body axes via a coordinate transformation. Then the converted noise is further processed via a GSE (Kalman Filter) for further noise reduction. The filtered noise (more precisely the attitude estimation error) is finally treated as measurement error input η_m in the closed-loop feedback system. It is thus turned into a PEC by applying the closed-loop transfer function matrix from measurement noise η_m to the control variable y (representing the pointing angles).

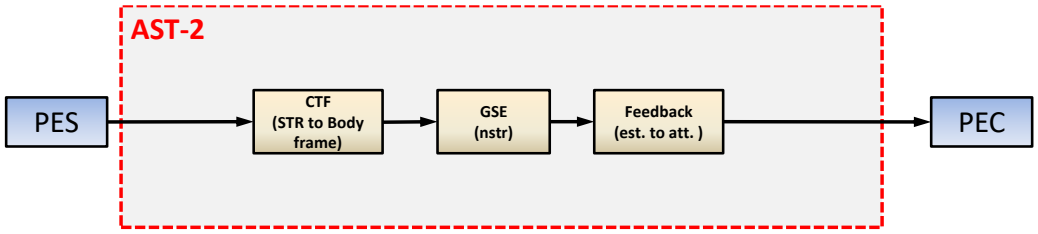

Figure 4-5: System transfer of PES 5 (according to AST-2 in [AD1])

4.1.6 PES 6: Star Tracker FOV and Pixel Spatial Errors

The PES itself describes another part of the unprocessed measurement noise of the star tracker in its sensor frame. Thus, it first has to be expressed in body axes via a coordinate transformation. Then the converted noise is further processed via an gyro-stellar estimator (Kalman Filter) for further noise reduction. The filtered noise (more precisely the attitude estimation error) is finally treated as measurement error input η_m in the closed-loop feedback system. It is thus turned into a PEC by applying the closed-loop transfer function matrix from measurement error η_m to the control variable y (representing the pointing angles).

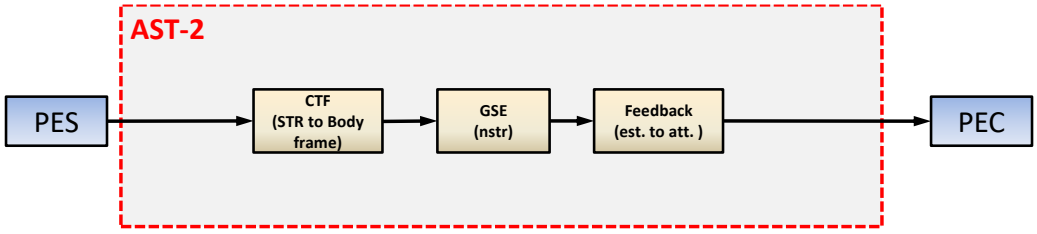

Figure 4-6: System transfer of PES 6 (according to AST-2 in [AD1])

4.1.7 PES 7: Gyro Noise

The PES itself describes the unprocessed measurement noise of the gyro assembly. This noise is first filtered and then processed via an estimator (Kalman Filter) for further noise reduction. The filtered noise is then treated as measurement error input η_m in the closed-loop feedback system (see section 4.2.9). It is thus turned into a PEC by applying the closed-loop transfer function matrix from measurement error η_m to the control variable y (representing the pointing angles).

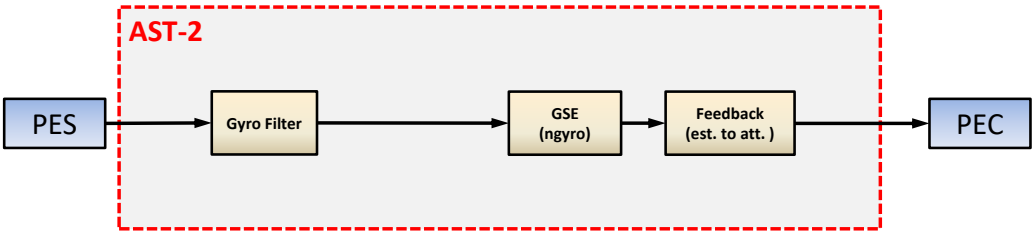

Figure 4-7: System transfer of PES 7 (according to AST-2 in [AD1])

4.1.8 PES 8: Cryocooler Micro-Vibrations

The PES describes the micro-vibrations at force level at the location of the cryocooler compressor. To convert these forces into an equivalent pointing error, the PES is input to a model representing the structural response of the satellite system in terms of pointing impact.

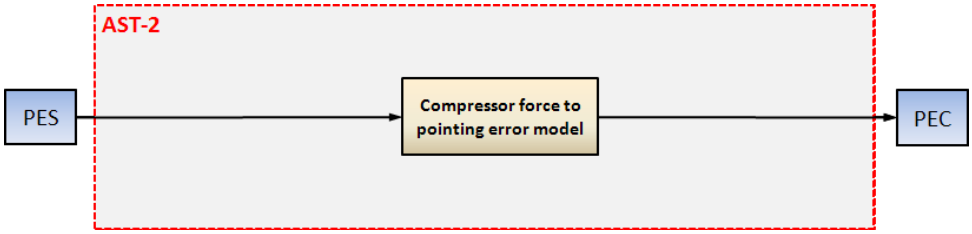

Figure 4-8: System transfer of PES 8 (according to AST-2 in [AD1])

4.1.9 PES 9 – PES11: Environmental disturbances

The environmental torques act on the satellite body and are counteracted by the AOCS. Using the common description of a closed-loop feedback system, PES 9 to PES11 act as a disturbance input η_d on the satellite plant. It is thus turned into a PEC by applying the closed-loop transfer function matrix from η_d to the control variable y (representing the pointing angles). Note that with release v1.1beta of PEET, drift signals are now approximated by a Fourier series. Therefore it is now possible to correctly transfer PES 10 through the feedback system, which was not possible before and had to be done in an extra analysis step outside of PEET, e.g. through time simulation.

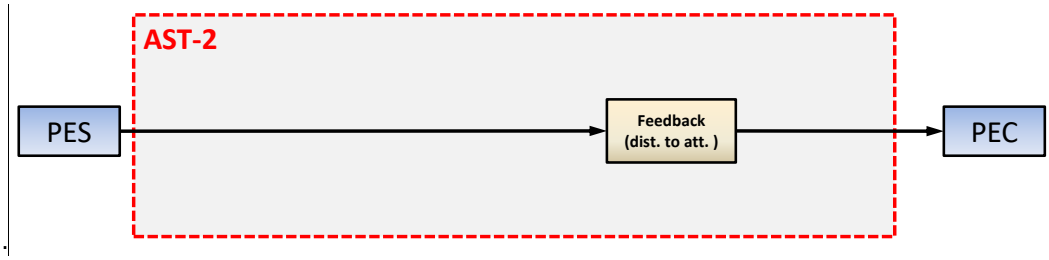

Figure 4-9: System transfer of PES 9 – PES 11 (according to AST-2 in [AD1])

4.1.10 PES 12: Thermo-Elastic Distortion (Periodic Part)

As the thermo-elastic distortion between payload and mounting plate of the star tracker directly affects the pointing error, no further system transfer is required, i.e. PES 12 directly represents a PEC.

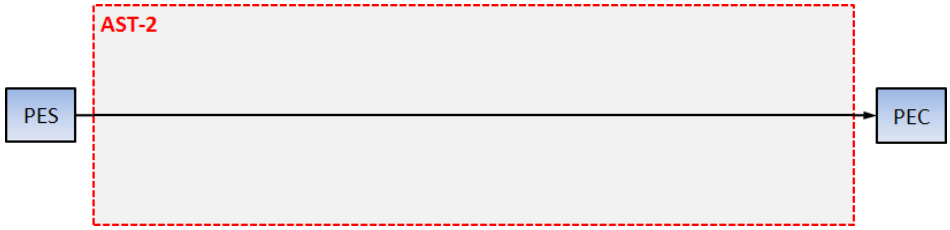

Figure 4-10: System transfer of PES 12 (according to AST-2 in [AD1])

4.1.11 PES 13: Thermo-Elastic Distortion (Transient Part)

As the thermo-elastic distortion between payload and mounting plate of the star tracker directly affects the pointing error, no further system transfer is required, i.e. PES 13 directly represents a PEC.

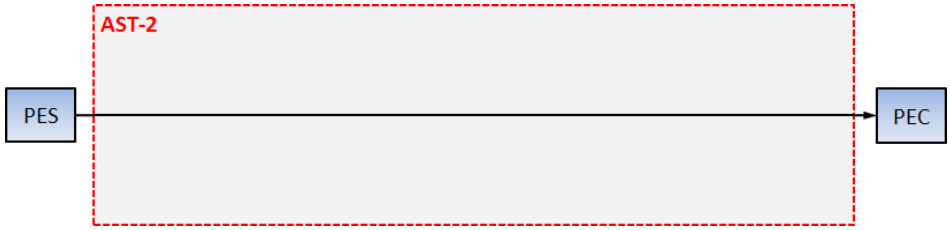

Figure 4-11: System transfer of PES 13 (according to AST-2 in [AD1])

4.1.12 PES 14: Thermo-Elastic Distortion (Random Part)

As the thermo-elastic distortion between payload and the mounting plate of the star tracker directly affects the pointing error, no further system transfer is required, i.e. PES 14 directly represents a PEC.

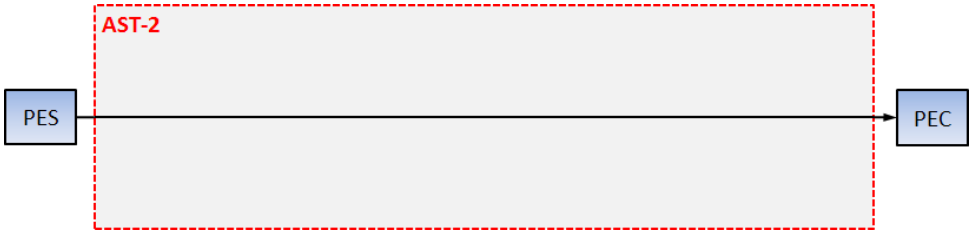

Figure 4-12: System transfer of PES 14 (according to AST-2 in [AD1])

4.1.13 PES 15: Star Tracker Internal Thermal Distortions

The internal thermo-elastic distortion of the STR describes another part of the unprocessed measurement error of the star tracker in its sensor frame. Thus, it first has to be expressed in body axes via a coordinate transformation. Then the converted error is further processed via an gyro-stellar estimator (Kalman Filter). The resulting attitude estimation error is finally treated as measurement error input η_m in the closed-loop feedback system. It is thus turned into a PEC by applying the closed-loop transfer function matrix from measurement error η_m to the control variable y (representing the pointing angles).

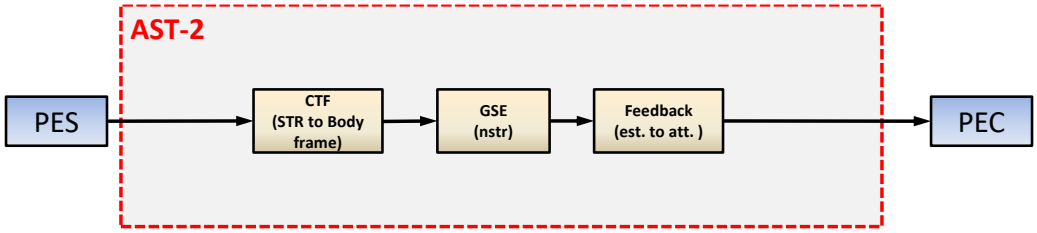

Figure 4-13: System transfer of PES 15 (according to AST-2 in [AD1])

4.1.14 PES 16: Thermal Stability Effect on Star Tracker

The PES describes the temperature stability at a location different from the required one. For that reason, the first step is to apply a thermal filter that describes the temperature transfer behaviour from the reference point on the optical bench interface to the star tracker camera head/detector. The converted temperature stability is an input for models describing the thermal noise impact on the detector, i.e. the induced measurement noise in the sensor frame. This noise has to be expressed subsequently in the

body frame before it is further processed in the attitude estimator. The residual noise is finally treated as measurement error input η_m in the closed-loop feedback system. It is thus turned into a PEC by applying the closed-loop transfer function matrix from measurement error η_m to the control variable y (representing the pointing angles).

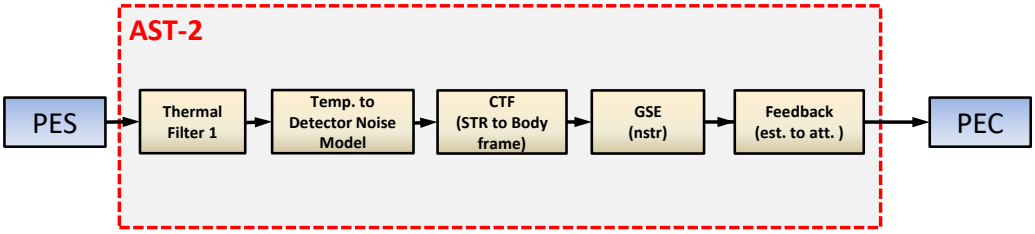

Figure 4-14: System transfer of PES 16 (according to AST-2 in [AD1])

4.1.15 PES 17: Thermal Stability Effect on Payload

Similar to PES 16 this PES describes the temperature stability at a location different from the required one. For that reason, the first step is to apply a thermal filter that describes the temperature transfer behaviour from the reference point on the optical bench interface to the structural parts affecting the focal point. The resulting temperature stability is input for a model describing the distortion impact of thermal noise on the focal point.

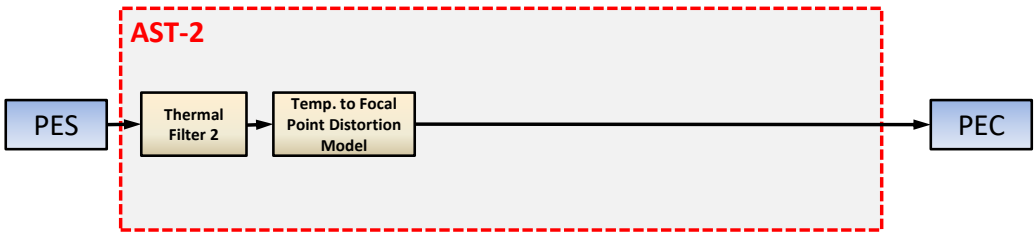

Figure 4-15: System transfer of PES 17 (according to AST-2 in [AD1])

4.1.16 PES 18: Station Keeping Manoeuvre Control Performance Error Transient

This pointing error source is formulated directly as a pointing performance error, hence no further system transfer is required and PES 18 directly represents a PEC System Transfer of PES 18(according to AST-2 in [AD1])

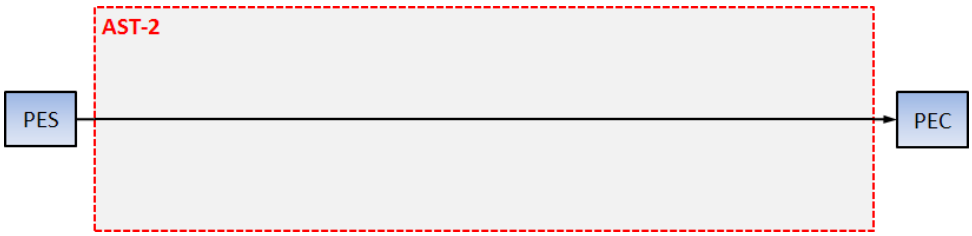

Figure 4-16 System Transfer of PES 18 (according to AST-2 in [AD1])

4.2 Transfer Model Definition

This chapter describes the applied models for the system transfer of the PES presented in the previous subsection (see also overview in Figure 4-21). The models are partially very simplified at the current stage and might be replaced in case more detailed descriptions become available.

4.2.1 Reaction wheel actuation matrix

The torque error (PES4) is available for a single RW around its spin axis. To convert the (identical) individual error to an equivalent torque error of the whole set of N_{rw} RWs, an actuation matrix A_{rw} of size N_{rw} x 3 is necessary which implicitly includes the orientation of each RW with respect to the spacecraft body frame. For the PointingSat example using 5 actuators, this actuation matrix is given by:

$$\mathbf{A}_{rw} = \begin{bmatrix} 0.7660 & 0 & 0.6428 \\ 0.7660 & 0.6040 & 0.2198 \\ 0.7660 & 0.6040 & -0.2198 \\ 0.7660 & -0.6040 & -0.2198 \\ 0.7660 & -0.6040 & 0.2198 \end{bmatrix} \qquad \text{Eq 4-1}$$

Using PEET the user defines this matrix by using the static system block “Mapping Matrix’, defining an input number of 5 (according to N_{rw}). Note that the PEET mapping block creates correlated output samples.

4.2.2 Coordinate Transformation (star tracker to body frame)

All coordinate transformations are defined in chapter 2.4. The only transformation needed is the one from the star tracker to the body frame of the system defined in chapter 2.4.6.4.

4.2.3 Gyro Rate Noise Filter

Due to the quantization error of the gyro rate noise model (PES7), the PSD increases linearly with higher frequencies. However this high frequency data is not used in the Gyro-Stellar Estimator and therefore a low-pass filter is implemented directly after PES7. This filter has a cut-off frequency of 0.25 Hz.

$$TF_{gyro,1} = \frac{4s+12}{8s^2+12s+12} \qquad \text{Eq 4-2}$$

4.2.4 Gyro-Stellar Estimator

Rate measurements of the gyroscopes and attitude measurements from the star tracker are filtered using a gyro-stellar estimator (basically a fixed-gain Kalman filter) to obtain an improved attitude estimate as well as a rate estimate.

Assuming a single-axis filter for each of the three body axes, the transfer function matrix for the estimation errors on each axis (which are fed to the PD controller) is given by (see [RD8]):

$$\begin{bmatrix} e_\varphi \\ e_\omega \end{bmatrix} = \frac{1}{s^2 + K_1 s - K_2} \begin{bmatrix} (K_1 s - K_2)\, e_\varphi + s\, e_\omega \\ -K_2 s\ e_\varphi + (s^2 + K_1 s)\, e_\omega \end{bmatrix} \quad \text{Eq 4-3}$$

where axis indices have been omitted. The inputs to the gyro-stellar estimator block are thus the star tracker noise contributions (from PES 3, 5, 6, 15 and 16) combined in n_{str} and the gyro noise n_{gyro} from PES7 (that implicitly includes drift bias noise as rate random walk contribution.

The Kalman gains[2] for the different axes are given by:

$$\mathbf{K}_1 = \begin{bmatrix} K_{1,x} \\ K_{1,y} \\ K_{1,z} \end{bmatrix} = \begin{bmatrix} 0.5 \\ 0.5 \\ 0.5 \end{bmatrix} \quad \text{Eq 4-4}$$

$$\mathbf{K}_2 = \begin{bmatrix} K_{2,x} \\ K_{2,y} \\ K_{2,z} \end{bmatrix} = -\begin{bmatrix} 0.1 \\ 0.1 \\ 0.1 \end{bmatrix} \quad \text{Eq 4-5}$$

4.2.5 Thermal Filters

For PES 16 and 17 only the thermal stability at a measurement point different from the required ones is available. The thermal filter models describe the transfer of the temperature stability via the spacecraft structure to the desired locations, namely the star tracker detector and payload telescope structure. Generally this information will be computed with complex FEM models.

For the PointingSat example, it is assumed that an approximate solution can be extracted from the complex model which can be characterized by a simple transfer function with low-pass behaviour. This low-pass is illustrated in Figure 4-17:

$$\mathrm{TF}_{\mathrm{thermal},1} = \frac{0.01257}{\mathrm{s} + 0.01257} \quad \text{Eq 4-6}$$

$$TF_{thermal,2} = \frac{3.142 \cdot 10^{-2}}{s + 3.142 \cdot 10^{-2}} \quad \text{Eq 4-7}$$

[2] Note that K_1 and K_2 correspond to the gains K_p and K_d (in this sequence) in the block mask dialog.

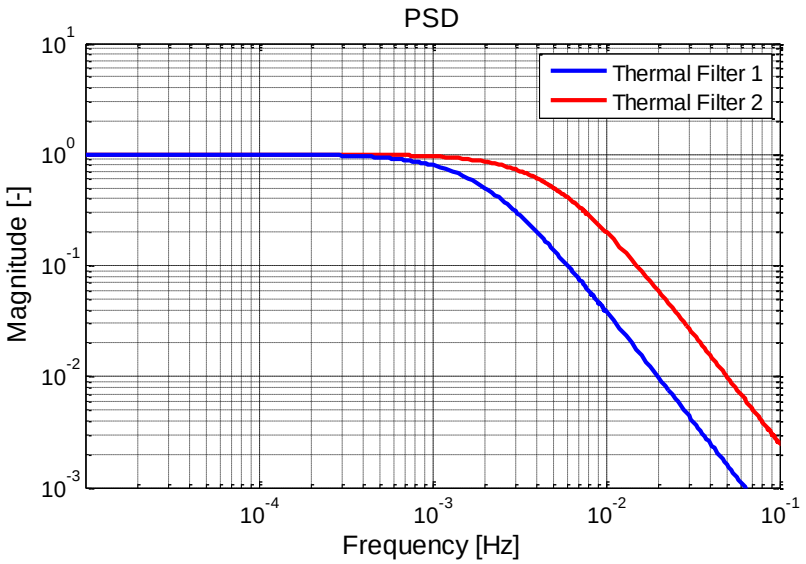

Figure 4-17: Thermal filter transfer functions for transfer of PES 16 and PES 17

This model can be realized in PEET by feeding the PES by a dynamic system block and defining above transfer functions on all main diagonals.

4.2.6 Temperature Stability to Detector Noise Model

Due to the lack of a more sophisticated model for the system transfer of PES 16 at current state, the impact of temperature stability on the noise of the star tracker is realized in a very simplified way.

The underlying assumption is that the temperature changes have approximately a linear effect on the detector due to thermal expansion. Some structural 'damping' of the temperature fluctuations generally exist which can be considered already treated by the applied thermal filters (section 4.2.5). The 'remainder' is then a static gain which gets directly mapped into attitude errors via a certain scaling factor.

This model is realized in PEET using a static system with the respective conversion gains $K_{11,ax}$ on the main diagonal:

$$\begin{bmatrix} K_{15,x} & 0 & 0 \\ 0 & K_{15,y} & 0 \\ 0 & 0 & K_{15,z} \end{bmatrix} \frac{\text{arcsec}}{K} = \begin{bmatrix} 1.34 & 0 & 0 \\ 0 & 1.34 & 0 \\ 0 & 0 & 0.65 \end{bmatrix} \frac{\text{arcsec}}{K} \qquad \text{Eq 4-8}$$

4.2.7 Temperature Stability to Focal Point Distortion Model

As for the system transfer of PES 16, no sophisticated model for the system transfer of PES 17 is available.

Assuming again the structural damping to be already covered by the thermal filter in section 4.2.5 and an approximately linear impact due to thermal expansion, the effect of the focal point distortion can be realized once more by a static system with conversion gains $K_{12,ax}$ on the main diagonal of the block:

$$\begin{bmatrix} K_{16,x} & 0 & 0 \\ 0 & K_{16,y} & 0 \\ 0 & 0 & K_{16,z} \end{bmatrix} \frac{\text{arcsec}}{K} = \begin{bmatrix} 0.89 & 0 & 0 \\ 0 & 1.16 & 0 \\ 0 & 0 & 1.19 \end{bmatrix} \frac{\text{arcsec}}{K} \qquad \text{Eq 4-9}$$

4.2.8 Compressor Force to Pointing Error Conversion

As for the temperature stability related effects, some kind of FEM model would be required for a detailed computation of the compressor forces transfer of PES 8 via the structure to an equivalent pointing error. For the PointingSat example it is assumed that this transfer behaviour can be sufficiently approximated transfer function of a spring-damper-system that accounts for the structural damping implicitly scaled by an additional conversion factor describing the relation between force and pointing, i.e.

$$TF_{structure} = \frac{K_8 \omega_0^2}{s^2 + 2\zeta\omega_0 s + \omega_0^2} \qquad \text{Eq 4-10}$$

Assuming a damping factor ζ=0.1, a structure eigenfrequency of 10 Hz and a conversion factor K_8 = 1.6 arcsec/N for the PointingSat example, the corresponding transfer function (identical for all axes) is shown in Figure 4-18 below.

The realization in PEET requires then the definition of above transfer function on the main diagonals of a dynamic system block.

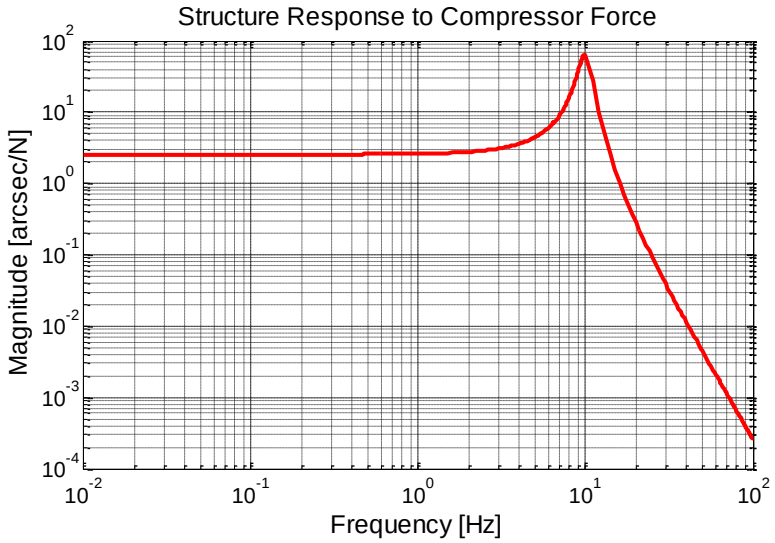

Figure 4-18: Structure Response to force loads

4.2.9 Feedback

Generally, any feedback system required for the system transfer could be realized by defining the respective closed-loop transfer function for each PES in a standard PEET ‘Dynamic System’ block. Assume that multiple PES have to be fed through the same feedback system but at different ‘input locations’ of the loop. In this case multiple ‘Dynamic System’ blocks are required and a modification of parameters in the feedback system would lead to a manual re-computation of the transfer function by the user with subsequent editing of multiple blocks.

To avoid such effort, the ‘Feedback’ block in PEET can be used to modify parameters directly with automatic update of the underlying closed-loop transfer function. Within the Container every other kind of transfer system blocks can be used to form the feedback system of interest.

4.2.9.1 Satellite plant model

The satellite plant is assumed to be a rigid body which is fully defined by its inertia for the pointing error evaluation purpose. Neglecting couplings between the body axes for the PointingSat example, the transfer function of the satellite plant (from torque to attitude) for axis ax is simply given by:

$$G = TF_{plant,ax} = \frac{1}{I_{ax,ax}\, s^2} \qquad \text{Eq 4-11}$$

where $I_{ax,ax}$ is the main diagonal element of the inertia tensor for axis ax. The inertia tensor for PointingSat is assumed as:

$$I = \begin{bmatrix} 4600 & 0 & 0 \\ 0 & 4300 & 0 \\ 0 & 0 & 1800 \end{bmatrix} kgm^2 \qquad \text{Eq 4-12}$$

4.2.9.2 Attitude controller

For the purpose of PointingSat, a simple SISO PD controller is used for attitude control separately for each body axes:

$$\mathrm{TF}_{\mathrm{ctrl.ax}} = \mathrm{K}_{\mathrm{P,ax}}\varphi_{\mathrm{ax}} + \mathrm{K}_{\mathrm{D,ax}}\omega_{\mathrm{ax}} \qquad \text{Eq 4-13}$$

$K_{P,ax}$ and $K_{D,ax}$ denote the proportional and derivative gains for the respective axis. Generally φ_{ax} describes the difference between desired attitude and attitude estimate from the gyro-stellar estimator (around axis ax) and ω_{ax} the difference between desired rate and measured rate around (around axis ax) corrected by the bias estimate from the gyro-stellar estimator, i.e. (axis index omitted):

$$\varphi = \varphi_{\mathrm{ref}} - \varphi_{\mathrm{est}} = \varphi_{\mathrm{ref}} - (\varphi_{\mathrm{real}} + \tilde{\varphi}) \qquad \text{Eq 4-14}$$

$$\omega = \omega_{\mathrm{ref}} - \omega_{\mathrm{est}} = \omega_{\mathrm{ref}} - (\omega_{\mathrm{real}} + \omega_{\mathrm{noise}} + \mathrm{B}_{\mathrm{real}} - (\mathrm{B}_{\mathrm{real}} + \tilde{\mathrm{B}})) \qquad \text{Eq 4-15}$$

As only error signals are relevant for the scope of pointing error analysis, it is not the ‘complete’ signal which has to be fed to the controller in the feedback block. These required signals are represented by the attitude and drift bias estimation error only, which are the output of the gyro-stellar estimation block (denoted with a “~” in the transfer functions in section 4.2.3) and the rate noise from PES 7:

$$\varphi = -\tilde{\varphi} \qquad \text{Eq 4-16}$$

$$\omega = -\omega_{\mathrm{noise}} + \tilde{\mathrm{B}} \qquad \text{Eq 4-17}$$

For the PointingSat example, the following controller gains are used and specified in the ‘PID Controller’ tab of the feedback block assuming a 0.08 Hz bandwidth of the attitude control:

$$\mathbf{K}_P = \begin{bmatrix} K_{P,x} \\ K_{P,y} \\ K_{P,z} \end{bmatrix} = -\begin{bmatrix} 581.23 \\ 543.97 \\ 227.71 \end{bmatrix} \quad \text{Eq 4-18}$$

$$\mathbf{K}_I = \begin{bmatrix} K_{I,x} \\ K_{I,y} \\ K_{I,z} \end{bmatrix} = \begin{bmatrix} 0 \\ 0 \\ 0 \end{bmatrix} \quad \text{Eq 4-19}$$

$$\mathbf{K}_D = \begin{bmatrix} K_{D,x} \\ K_{D,y} \\ K_{D,z} \end{bmatrix} = -\begin{bmatrix} 1976.2 \\ 1849.5 \\ 774.2 \end{bmatrix} \quad \text{Eq 4-20}$$

The overall transfer function of the SISO-PID controller for each axis is given by:

$$K = K_P + \frac{K_I}{s} + K_D s \quad \text{Eq 4-21}$$

4.2.9.3 Loop structure

If the PID controller input would only be dependent on a single source (i.e. attitude estimation error from GSE only), the setup of the simple loop structure shown in Figure 4-19 below would be a sufficient model.

It consists of a PID controller K and a rigid body plant model G (with the parameters defined in the previous subsections) with PES acting on the disturbance (η_d) and measurement error (η_m) inputs and affecting the pointing output y (=φ in this case).

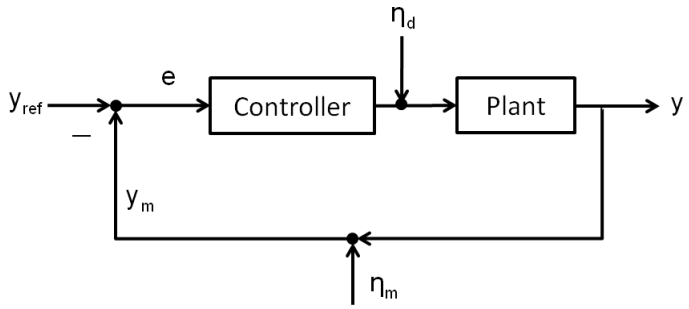

Figure 4-19: Feedback loop structure (attitude noise input only)

For the PointingSat example a more complex loop scheme is required as the controller input not only comprises attitude information as single source, but also rate information. Generally, this would require an inner loop for the rate feedback (see figure below) while nested loops are supported within the container block in PEET.

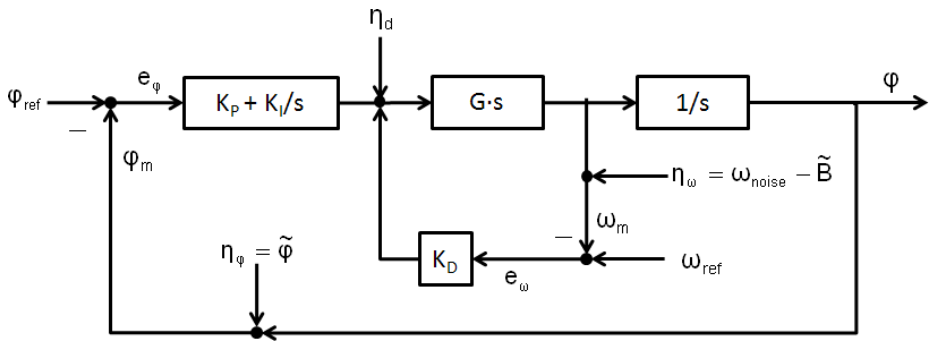

Figure 4-20: Feedback loop structure (with attitude and rate noise input)

The input parameters to the container, which contains the loop depicted in Figure 4-20, are the following:

- φ_{ref} as reference attitude angle. For the determination of the pointing error the reference is set to zero.
- η_d as disturbance torques represented by the RW torque errors (PES4) and the environmental disturbances (PES9 – PES11).
- η_ω as gyro rate noise represented by the gyro noise error source PES7.
- η_φ as attitude estimation represented by the output signal of the gyro stellar estimator.
- ω_{ref} as reference angular rate. For the determination of the pointing error this value is set to zero.

The output parameter of the container is the error of φ, denoted as $e_\varphi = \varphi - \varphi_{ref}$. Due to the fact that the reference is set to zero, the output is $e_\varphi = \varphi$.

4.3 PointingSat realization in the PEET

There are multiple ways of setting up the previously described pointing system in PEET. One possible realization of the overall PES and system transfer is shown in Figure 4-21, which is the most ‘compact’ one in terms of block usage.

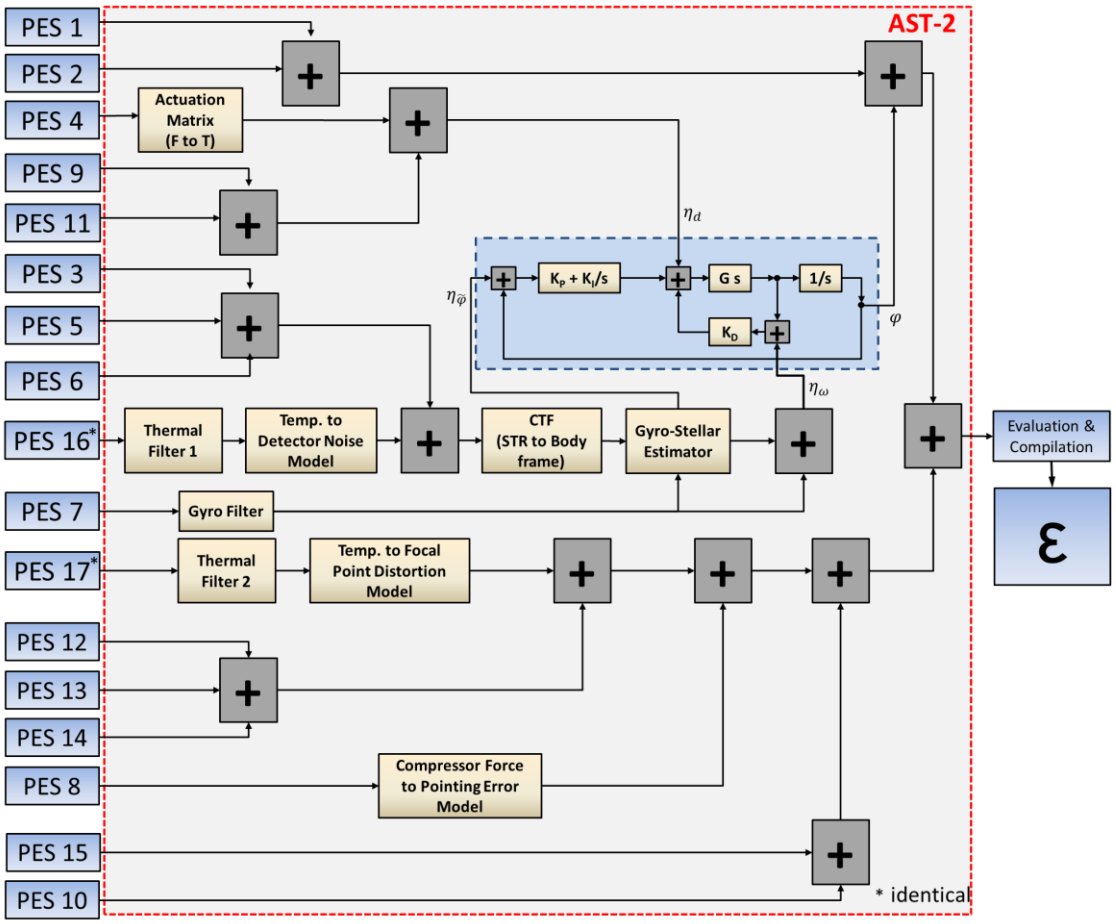

Figure 4-21: Compact realization of PointingSat Case Study

An alternative setup is shown in Figure 4-22. It follows a ‘parallel’ approach with one final summation after all system transfers. This setup could simplify the determination of the driving PES as the individual contributions can directly be compared at the input ports of the summation block in the PEET tree view. A possible disadvantage of the parallel approach is the multiple use of identical blocks: This complicates quick changes of the system structure or may result in larger computation times due to the larger number of signals to be computed.

The actual implementation of the PointingSat case study follows a ‘mixed’ approach and makes use of the possibility to group several PES into subsystems. As shown in Figure 4-23, the PES are grouped into three parallel subsystems. The realization within each subsystem may be compact or parallel and could also include further levels of sub-subsystems etc. For instance, the “Platform” subsystem contains the “performanceErr” and “knowledgeErr” subsystems, where the former’s implementation follows the compact approach (see Figure 4-24). This logical structuring allows a quick error evaluation on each level by analysing the input ports of the respective summation blocks.

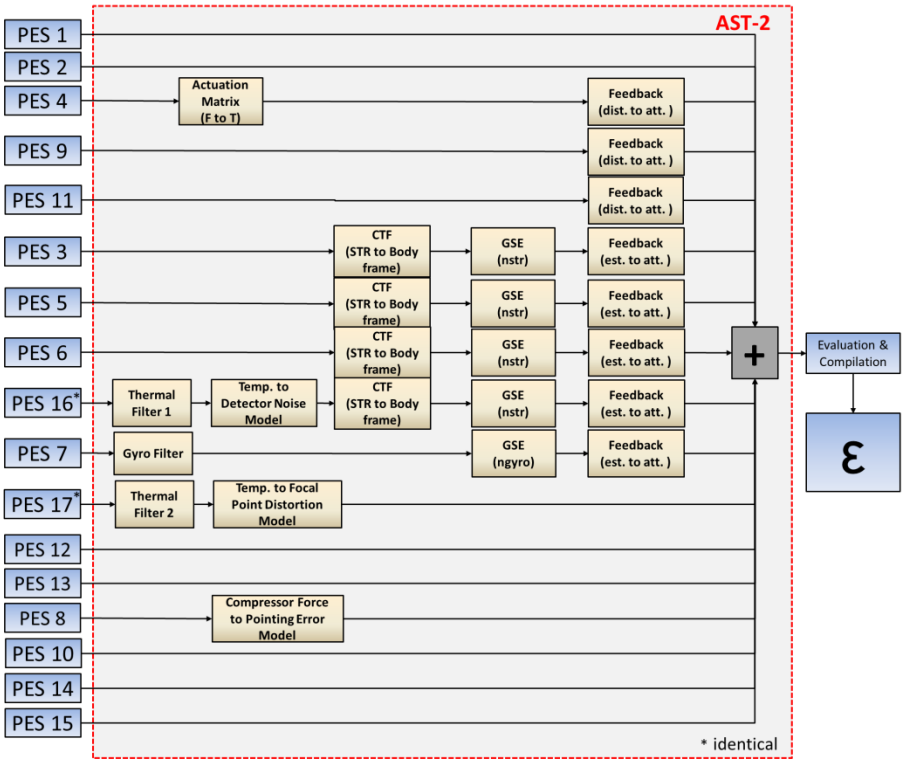

Figure 4-22: Parallel realization of PointingSat Case Study

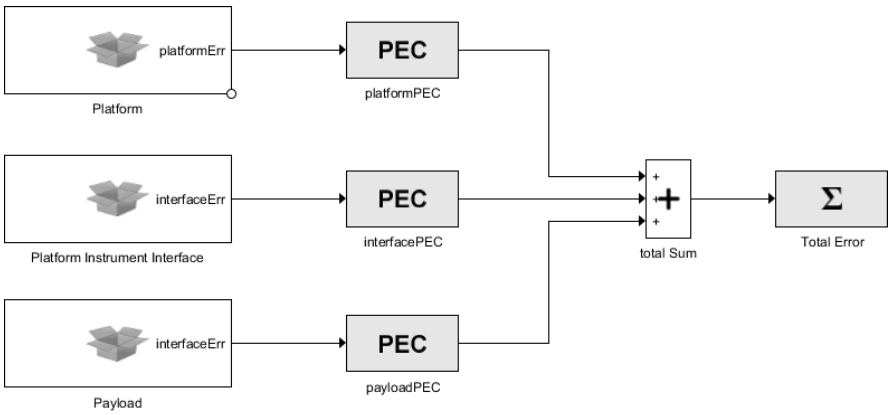

Figure 4-23: PointingSat Implementation in PEET: Top Level

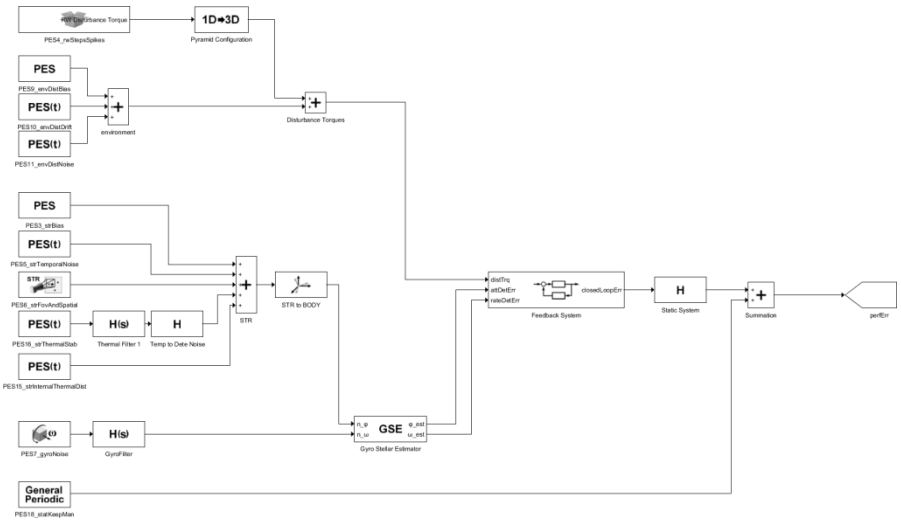

Figure 4-24: Compact Implementation of the Platform/PerformanceErr Block

5 Pointing Error Index Contribution (AST-3)

This section briefly describes the time-windowed pointing error index contribution analysis for the PointingSat example in accordance to AST-3 in [AD1]. This step is mainly related to the application of the pointing error metrics which are dependent on the error index under consideration.

For all PES (more precisely PEC at this point) which are described as random process this is realized via pointing error metric weighting functions (Table 10-3 in [AD1]). In case of a time-random variable description of the PEC, the tables in appendix B of [AD2] are applied. While the latter represents only an approximation of the error contribution, the random process analysis is exact. Consequently, random process description of the PES/PEC should be preferred when sufficient data is available.

The contribution analysis is done automatically in PEET for all time-random PEC (as the time-constant ones do not contribute by definition).

AST-3 includes also the statistical interpretation of PEC which originates from RP type PES. This interpretation at PEC level will be highlighted in the following subsections for a representative set of distributions of the defined PES of PointingSat. The statements about the statistical interpretation are in line with the descriptions given in [AD2].

Note: Using PEET the user would only have to define a PES as described in chapter 3 further interpretation is performed automatically for the user-selected statistical interpretation and error index.

Note: The domain treatment worst-case in the ensemble domain and temporal domain is not defined in [AD1] and [AD2]. Furthermore there is not real evaluation of the underlying PDF possible in this case. This evaluation always results in a Dirac-delta function.

5.1 Statistical Interpretation of Constant Random Variable PES

5.1.1 Uniform Ensemble Distribution

PES3 is chosen as a representation of the Uniform distribution for the illustration of the statistical interpretation. See chapter 3.1.3.2 for the model definition.

- **APE / AKE:**

The statistical interpretation of this PES representation is demonstrated for the AKE and APE requirement in Table 5-1. The following interpretations are possible:

- Statistical evaluation of ensemble domain and worst-case evaluation of temporal domain: In this case the PES can directly be described by the underlying PDF. This results as there is no temporal-distribution and therefore there is no worst-case evaluation possible.
- Statistical evaluation of temporal domain and worst-case evaluation of ensemble domain: As the PES is time-constant, in case of this evaluation the worst-case ‘bias’ of the ensemble has to be taken into account.
- Statistical evaluation of both domains: As there is no temporal distribution (time-constant PES), this evaluation reduces to the case of statistical evaluation of the ensemble domain and worst-case evaluation of temporal domain.

- Worst-case evaluation of both domains: The worst-case evaluation results in the highest values of the ensemble-domain. Due to the limits of the uniform distribution this is represented by the upper bound.

Table 5-1: Statistical Interpretation of APE / AKE for Uniform PES type CRV

		Temporal domain	
		statistical	worst-case
Ensemble domain	statistical	$\boldsymbol{\alpha}_{3,SI} = \begin{bmatrix} \delta\left(U\left(0,\alpha_{3,\max,x}\right)\right) \\ \delta\left(U\left(0,\alpha_{3,\max,y}\right)\right) \\ \delta\left(U\left(0,\alpha_{3,\max,z}\right)\right) \end{bmatrix}$	$\boldsymbol{\alpha}_{3,SI} = \begin{bmatrix} \delta\left(U\left(0,\alpha_{3,\max,x}\right)\right) \\ \delta\left(U\left(0,\alpha_{3,\max,y}\right)\right) \\ \delta\left(U\left(0,\alpha_{3,\max,z}\right)\right) \end{bmatrix}$
	worst-case	$\boldsymbol{\alpha}_{3,SI} = \begin{bmatrix} \delta\left(\alpha_{3,\max,x}\right) \\ \delta\left(\alpha_{3,\max,y}\right) \\ \delta\left(\alpha_{3,\max,z}\right) \end{bmatrix}$	$\boldsymbol{\alpha}_{3,SI} = \begin{bmatrix} \delta\left(\alpha_{3,\max,x}\right) \\ \delta\left(\alpha_{3,\max,y}\right) \\ \delta\left(\alpha_{3,\max,z}\right) \end{bmatrix}$

- **RPE:**

As the PES is time-constant, it has no influence on the error index (see [AD2]). The PES reduces in every evaluation type to:

$$\boldsymbol{\alpha}_{3,SI} = \begin{bmatrix} \delta(0) \\ \delta(0) \\ \delta(0) \end{bmatrix} \qquad \text{Eq 5-1}$$

- **WPD:**

As the PES is time-constant, it has no influence on the error index (see [AD2]). The PES reduces in every evaluation type to eq.5-1.

- **WPR:**

As the PES is time-constant, it has no influence on the error index (see [AD2]). The PES reduces in every evaluation type to eq.5-1.

- **PDE:**

As the PES is time-constant, it has no influence on the error index (see [AD2]). The PES reduces in every evaluation type to eq.5-1.

5.1.2 Gaussian Ensemble Distribution

PES9 is chosen as a representation of the Gaussian distribution for the illustration of the statistical interpretation. See chapter 3.3.1.2 for the model definition. Note that the Gaussian distribution has no boundaries. Therefore the worst-case of this distribution is determined as 3σ value.

- **APE / AKE:**

The statistical interpretation of this PES representation is demonstrated for the AKE and APE requirement in Table 5-2. The following interpretations are possible:

- Statistical evaluation of ensemble domain and worst-case evaluation of temporal domain: In this case the PES can directly be described by the underlying PDF. This results as there is no temporal-distribution and therefore there is no worst-case evaluation possible.
- Statistical evaluation of temporal domain and worst-case evaluation of ensemble domain: As the PES is time-constant, in case of this evaluation the worst-case bias of the ensemble is taken into account. Due to the Gaussian ensemble distribution the 3σ value around the mean value is chosen.
- Statistical evaluation of both domains: As there is no temporal distribution (time-constant PES), this evaluation reduces to the case of statistical evaluation of the ensemble domain and worst-case evaluation of temporal domain.
- Worst-case evaluation of both domains: The worst-case evaluation results in the highest values of the ensemble-domain. Due to the Gaussian distribution this is represented by the 3σ value around the mean value.

Table 5-2: Statistical Interpretation of APE / AKE for Gaussian PES type CRV

		Temporal domain	
		statistical	worst-case
Ensemble domain	statistical	$\boldsymbol{\alpha}_{9,SI} = \begin{bmatrix} \delta\left(G\left(\mu_{9,x},\sigma_{9,x}\right)\right) \\ \delta\left(G\left(\mu_{9,y},\sigma_{9,x}\right)\right) \\ \delta\left(G\left(\mu_{9,z},\sigma_{9,z}\right)\right) \end{bmatrix}$	$\boldsymbol{\alpha}_{9,SI} = \begin{bmatrix} \delta\left(G\left(\mu_{9,x},\sigma_{9,x}\right)\right) \\ \delta\left(G\left(\mu_{9,y},\sigma_{9,x}\right)\right) \\ \delta\left(G\left(\mu_{9,z},\sigma_{9,z}\right)\right) \end{bmatrix}$
	worst-case	$\boldsymbol{\alpha}_{9,SI} = \begin{bmatrix} \delta(\lvert\mu_{9,x}\rvert + 3\cdot\sigma_{9,x}) \\ \delta(\lvert\mu_{9,y}\rvert + 3\cdot\sigma_{9,y}) \\ \delta(\lvert\mu_{9,z}\rvert + 3\cdot\sigma_{9,y}) \end{bmatrix}$	$\boldsymbol{\alpha}_{9,SI} = \begin{bmatrix} \delta(\lvert\mu_{9,x}\rvert + 3\cdot\sigma_{9,x}) \\ \delta(\lvert\mu_{9,y}\rvert + 3\cdot\sigma_{9,y}) \\ \delta(\lvert\mu_{9,z}\rvert + 3\cdot\sigma_{9,y}) \end{bmatrix}$

- **RPE:**

As the PES is time-constant, it has no influence on the error index (see [AD2]). The PES reduces in every evaluation type to:

$$\boldsymbol{\alpha}_{3,SI} = \begin{bmatrix} \delta(0) \\ \delta(0) \\ \delta(0) \end{bmatrix} \qquad \text{Eq 5-2}$$

- **WPD:**

As the PES is time-constant, it has no influence on the error index ([RD10]). The PES reduces in every evaluation type to eq.5-2.

- **WPR:**

As the PES is time-constant, it has no influence on the error index ([RD10]). The PES reduces in every evaluation type to eq.5-2.

- **PDE:**

As the PES is time-constant, it has no influence on the error index (see [AD2]). The PES reduces in every evaluation type to eq.5-2.

5.2 Statistical Interpretation of Random Variable PES

PES14 is chosen as a representation of the time-random variable for the illustration of the statistical interpretation. See chapter 3.3.6.2 for the model definition. Note that the Gaussian distribution has no boundaries. Therefore the worst-case of this distribution is determined as 3σ value.

- **APE / AKE:**

The statistical interpretation of this PES representation is demonstrated for the AKE and APE requirement in Table 5-3. The following interpretations are possible:

- Statistical evaluation of ensemble domain and worst-case evaluation of temporal domain: In case of this evaluation the time-random behaviour of the RV type PES is irrelevant and reduces to a Dirac-Delta function. Only the ensemble distribution is of interest.
- Statistical evaluation of temporal domain and worst-case evaluation of ensemble domain: In case of a description in terms of RV type, the PES can be described using the worst-case standard deviation of the underlying ensemble distribution. As the ensemble is uniformly distributed, the upper bound of this distribution is taken.
- Statistical evaluation of both domains: In this case the conditional probability has to be taken into account as stated in [AD2] Table B-3.
- Worst-case evaluation of both domains: For this evaluation the highest ensemble distribution value is chosen for the temporal distribution. With this value the worst-case temporal value is determined. Due to the Gaussian temporal distribution this is represented by the 3σ value around the mean value (which is zero in this case).

Table 5-3: Statistical Interpretation of APE / AKE for Gaussian PES type RV

	Temporal domain	
	statistical	worst-case

Ensemble domain	statistical	$\boldsymbol{\alpha}_{14,SI} = \begin{bmatrix} \int G(0,\sigma_{14,x})\, U(\sigma_{14,\min,x},\sigma_{14,\max,x})\mathrm{d}\sigma_{14,x} \\ \int G(0,\sigma_{14,y})\, U(\sigma_{14,\min,y},\sigma_{14,\max,y})\mathrm{d}\sigma_{14,y} \\ \int G(0,\sigma_{14,z})\, U(\sigma_{14,\min,z},\sigma_{14,\max,z})\mathrm{d}\sigma_{14,z} \end{bmatrix}$	$\boldsymbol{\alpha}_{14,SI} = \begin{bmatrix} \delta(U(\sigma_{14,\min,x},\sigma_{14,\max,x})) \\ \delta(U(\sigma_{14,\min,y},\sigma_{14,\max,y})) \\ \delta(U(\sigma_{14,\min,z},\sigma_{14,\max,z})) \end{bmatrix}$
	worst-case	$\boldsymbol{\alpha}_{14,SI} = \begin{bmatrix} G(0,\sigma_{14,\max,x}) \\ G(0,\sigma_{14,\max,y}) \\ G(0,\sigma_{14,\max,z}) \end{bmatrix}$	$\boldsymbol{\alpha}_{14,SI} = \begin{bmatrix} \delta(3\cdot\sigma_{14,\max,x}) \\ \delta(3\cdot\sigma_{14,\max,y}) \\ \delta(3\cdot\sigma_{14,\max,z}) \end{bmatrix}$

- **RPE:**

As PES14 is defined as zero-mean random variable, the evaluation is due to [AD2] table B-3 equal to the APE evaluation. Therefore the results of Table 5-3 apply also for the RPE error index.

- **WPD:**

From [RD10], Table A-4, there is no linear slope, hence there is no contribution to the WPD.

- **WPR:**

As there is no linear slope, hence the WPR equals the RPE, for which the results of Table 5-3 apply.

- **PDE:**

By definition in [AD2] table B-3, a Gaussian temporal distributed random variable does not contribute to the PDE error index. Additionally the ensemble distribution does not influence the contribution. Hence the PES reduces in every evaluation type to

$$\boldsymbol{\alpha}_{14,SI} = \begin{bmatrix} \delta(0) \\ \delta(0) \\ \delta(0) \end{bmatrix} \qquad \text{Eq 5-3}$$

5.3

5.3

5.3 Statistical Interpretation of Random Processes

PES16 is chosen as a representation of the random process for the illustration of the statistical interpretation. See chapter 3.3.8.2 for the model definition.

APE / AKE:

The statistical interpretation of this PES representation is demonstrated for the AKE and APE requirement in Table 5-4. The following interpretations are possible. Note that a PES type random process is always

described by a zero-mean Gaussian temporal distribution with a standard deviation equal to the one computed for the applied PSD.

- Statistical evaluation of ensemble domain and worst-case evaluation of temporal domain: The time-random behaviour of the underlying process is irrelevant. Hence only the maximum noise value has to be taken into account which is represented by the 3σ value of the Gaussian distribution.
- Statistical evaluation of temporal domain and worst-case evaluation of ensemble domain: This PES can be described by the underlying Gaussian distribution.
- Statistical evaluation of both domains: This case corresponds to the case of statistical evaluation of the temporal domain and worst-case evaluation of the ensemble domain.
- Worst-case evaluation of both domains: There are no ensemble realizations available for a PES type random process. Hence this case reduces to the statistical evaluation of the ensemble domain and worst-case evaluation of the temporal-domain.

Table 5-4: Statistical Interpretation of APE / AKE for PES type random process

		Temporal domain	
		statistical	worst-case
Ensemble domain	statistical	$\boldsymbol{\alpha}_{16,SI} = \begin{bmatrix} G\left(0,\sigma_{16,x}\right) \\ G\left(0,\sigma_{16,x}\right) \\ G\left(0,\sigma_{16,x}\right) \end{bmatrix}$	$\boldsymbol{\alpha}_{16,SI} = \begin{bmatrix} \delta\left(3\cdot\sigma_{16,x}\right) \\ \delta\left(3\cdot\sigma_{16,y}\right) \\ \delta\left(3\cdot\sigma_{16,z}\right) \end{bmatrix}$
	worst-case	$\boldsymbol{\alpha}_{16,SI} = \begin{bmatrix} G\left(0,\sigma_{16,x}\right) \\ G\left(0,\sigma_{16,x}\right) \\ G\left(0,\sigma_{16,x}\right) \end{bmatrix}$	$\boldsymbol{\alpha}_{16,SI} = \begin{bmatrix} \delta\left(3\cdot\sigma_{16,x}\right) \\ \delta\left(3\cdot\sigma_{16,y}\right) \\ \delta\left(3\cdot\sigma_{16,z}\right) \end{bmatrix}$

- **RPE, WPD, WPR and PDE:**

The rules for the statistical interpretation as given in Table 5-4 apply to all error indices, also for the RPE, WPD, WPR and PDE. For the error index evaluation however there are exact rules due to the frequency information delivered in the PSD. Hence metric weighting filter can be applied to characterize the specifics of the error index. Thus the derived rules for the statistical interpretation are applied on the standard deviation as derived by the error index filtering.

5.4 Statistical Interpretation of Periodic PES

PES8 is chosen as a representation of the periodic PES for the illustration of the statistical interpretation. See chapter 3.2.5.2 for the model definition.

- **APE / AKE:**

The statistical interpretation of this PES representation is demonstrated for the AKE and APE requirement in Table 5-5. The following interpretations are possible. Note that a PES type periodic is always described by a bimodal temporal distribution with the bimodal factor equal to the amplitude of the periodic signal.

- Statistical evaluation of ensemble domain and worst-case evaluation of temporal domain: The PES has to be described by worst-case amplitudes at each frequency. With the applied ensemble distribution, this collapses to a Dirac-Delta function of a Uniform distribution.
- Statistical evaluation of temporal domain and worst-case evaluation of ensemble domain: The PES can be described by a bimodal distribution characterized by discrete amplitudes. These amplitudes are the worst-case amplitudes over the ensemble, which is represented by the upper bound of the Uniform ensemble distribution.
- Statistical evaluation of both domains: In this case the conditional probability of the ensemble and the temporal distribution has to be taken into account.
- Worst-case evaluation of both domains: The worst-case amplitude over the ensemble is chosen, which the upper bound of the Uniform ensemble distribution is. Furthermore the Bimodal temporal distribution decreases to a Dirac-Delta function.

Table 5-5: Statistical Interpretation of APE / AKE for PES type periodic

		Temporal domain	
		statistical	worst-case
Ensemble domain	statistical	$\boldsymbol{\alpha}_{8,SI} = \begin{bmatrix} \int BM\left(\mathbf{A}_{8,x}\right) U\left(\mathbf{A}_{8,x,\min}, \mathbf{A}_{8,x,\max}\right) \mathrm{d}\mathbf{A}_{8,x} \\ \int BM\left(\mathbf{A}_{8,y}\right) U\left(\mathbf{A}_{8,y,\min}, \mathbf{A}_{8,y,\max}\right) \mathrm{d}\mathbf{A}_{8,y} \\ \int BM\left(\mathbf{A}_{8,z}\right) U\left(\mathbf{A}_{8,z,\min}, \mathbf{A}_{8,z,\max}\right) \mathrm{d}\mathbf{A}_{8,z} \end{bmatrix}$	$\boldsymbol{\alpha}_{8,SI} = \begin{bmatrix} \delta\left(U\left(\mathbf{A}_{8,x,\min}, \mathbf{A}_{8,x,\max}\right)\right) \\ \delta\left(U\left(\mathbf{A}_{8,y,\min}, \mathbf{A}_{8,y,\max}\right)\right) \\ \delta\left(U\left(\mathbf{A}_{8,z\min}, \mathbf{A}_{8,z,\max}\right)\right) \end{bmatrix}$
	worst-case	$\boldsymbol{\alpha}_{8,SI} = \begin{bmatrix} BM\left(\mathbf{A}_{8,x,\max}\right) \\ BM\left(\mathbf{A}_{8,y,\max}\right) \\ BM\left(\mathbf{A}_{8,z,\max}\right) \end{bmatrix}$	$\boldsymbol{\alpha}_{8,SI} = \begin{bmatrix} \delta\left(\mathbf{A}_{8,x,\max}\right) \\ \delta\left(\mathbf{A}_{8,y,\max}\right) \\ \delta\left(\mathbf{A}_{8,z,\max}\right) \end{bmatrix}$

- **RPE, WPD, WPR and PDE:**

The rules for the statistical interpretation as given in Table 5-5 apply to all error indices, also for the RPE, WPD, WPR and PDE. For the error index evaluation however there are exact rules due to the frequency information delivered in the amplitude spectrum of the periodic signal. Hence the values of the metric weighting filter at the frequency of the PES can be applied to characterize the specifics of the error index. Thus the statistical interpreted amplitude is multiplied by this weighting factor for the index evaluation.

5.5 Statistical Interpretation of Drift PES

From PEET V1.1 onwards, drift errors are modelled as a Fourier series approximation which allows applying the exact signal domain metrics available for periodic signals. Thus, their evaluation is

equivalent to those described in section 5.3 and 5.4. For completeness, the evaluation for the former random variable approach is described below.

PES10 is chosen as a representation of the Drift for the illustration of the statistical interpretation. See chapter 3.3.2.2 for the model definition.

- **APE / AKE**:

The statistical interpretation of this PES representation is demonstrated for the AKE and APE requirement in . The following interpretations are possible. Note that a PES type Drift has always a Uniform temporal distribution with the range from zero to the highest amplitude of the drift (rate multiplied by reset time).

- Statistical evaluation of ensemble domain and worst-case evaluation of temporal domain: Due to the Uniform temporal distribution, the PDF reduces to the upper bound of this distribution. This bound is only described by the ensemble distribution.
- Statistical evaluation of temporal domain and worst-case evaluation of ensemble domain: With above described transformation to a Uniform temporal distribution, the worst-case ensemble distribution has to be taken for the upper bound. Therefore the Gaussian distribution, respective its 3σ value is taken into account.
- Statistical evaluation of both domains: In this case the conditional probability has to be taken into account as stated in [AD2] Table B-4.
- Worst-case evaluation of both domains: This case uses the worst-case of the Gaussian ensemble distribution which is represented by the 3σ value. This value is used in the worst-case temporal distribution. Therefore the upper bound of the Uniform PDF is taken into account.

Table 5-6: Statistical Interpretation of APE / AKE for PES type Drift

		Temporal domain	
		statistical	worst-case
Ensemble domain	statistical	$\boldsymbol{\varepsilon}_{D,10,SI} = \begin{bmatrix} \int U\left(0, \Delta t_{10,D} \cdot \sigma_{10,x}\right) G\left(0, \sigma_{10,x}\right) \\ \int U\left(0, \Delta t_{10,D} \cdot \sigma_{10,y}\right) G\left(0, \sigma_{10,y}\right) \\ \int U\left(0, \Delta t_{10,D} \cdot \sigma_{10,z}\right) G\left(0, \sigma_{10,z}\right) \end{bmatrix}$	$\boldsymbol{\varepsilon}_{D,10,SI} = \begin{bmatrix} \delta\left(\Delta t_{10,D} \cdot G\left(0, \sigma_{10,x}\right)\right) \\ \delta\left(\Delta t_{10,D} \cdot G\left(0, \sigma_{10,y}\right)\right) \\ \delta\left(\Delta t_{10,D} \cdot G\left(0, \sigma_{10,z}\right)\right) \end{bmatrix}$
	worst-case	$\boldsymbol{\varepsilon}_{D,10,SI} = \begin{bmatrix} U\left(0, \Delta t_{10,D} \cdot 3 \cdot \sigma_{10,x}\right) \\ U\left(0, \Delta t_{10,D} \cdot 3 \cdot \sigma_{10,y}\right) \\ U\left(0, \Delta t_{10,D} \cdot 3 \cdot \sigma_{10,z}\right) \end{bmatrix}$	$\boldsymbol{\varepsilon}_{D,10,SI} = \begin{bmatrix} \delta\left(\Delta t_{10,D} \cdot 3 \cdot \sigma_{10,x}\right) \\ \delta\left(\Delta t_{10,D} \cdot 3 \cdot \sigma_{10,y}\right) \\ \delta\left(\Delta t_{10,D} \cdot 3 \cdot \sigma_{10,z}\right) \end{bmatrix}$

- **RPE:**

The statistical interpretation of this PES representation is demonstrated for the RPE requirement in . The following interpretations are possible. Note that a PES type Drift has always a Uniform temporal distribution with the range from zero to the highest amplitude of the drift (rate multiplied by reset time).

- Statistical evaluation of ensemble domain and worst-case evaluation of temporal domain: The temporal distribution reduces to a Dirac-Delta function due to its worst-case evaluation. As stated in [AD2] this distribution does not contribute to the RPE error index.
- Statistical evaluation of temporal domain and worst-case evaluation of ensemble domain: The RPE error index always refers to the mean value over a time-window. Hence a Uniform distribution within this time-window and with the respective ensemble worst-case drift rate is taken into account.
- Statistical evaluation of both domains: In this case the conditional probability has to be taken into account as stated in [AD2] Table B-4.
- Worst-case evaluation of both domains: The temporal distribution reduces to a Dirac-Delta function due to its worst-case evaluation. As stated in [AD2] this distribution does not contribute to the RPE error index.

- **WPD:**

According to [RD10], Table A-14, the RPE consists entirely of the WPD for a drift type PES. Therefore, the discussion in the previous paragraph applies.

- **WPR:**

As the RPE consists entirely of the WPD, there is no contribution to the WPR.

- Table 5-7: Statistical Interpretation of RPE for PES type Drift

		Temporal domain	
		statistical	worst-case
Ensemble domain	statistical	$\boldsymbol{\varepsilon}_{D,10,SI} = \begin{bmatrix} \int U\left(-0.5\cdot\Delta T\cdot\sigma_{10,x}, 0.5\cdot\Delta T\cdot\sigma_{10,x}\right) G\left(0,\sigma_{10,x}\right) \\ \int U\left(-0.5\cdot\Delta T\cdot\sigma_{10,x}, 0.5\cdot\Delta T\cdot\sigma_{10,x}\right) G\left(0,\sigma_{10,y}\right) \\ \int U\left(-0.5\cdot\Delta T\cdot\sigma_{10,x}, 0.5\cdot\Delta T\cdot\sigma_{10,x}\right) G\left(0,\sigma_{10,z}\right) \end{bmatrix}$	$\boldsymbol{\varepsilon}_{D,10,SI} = \begin{bmatrix} \delta(0) \\ \delta(0) \\ \delta(0) \end{bmatrix}$
	worst-case	$\boldsymbol{\varepsilon}_{D,10,SI} = \begin{bmatrix} U\left(-1.5\cdot\Delta T\cdot\sigma_{10,x}, 1.5\cdot\Delta T\cdot\sigma_{10,x}\right) \\ U\left(-1.5\cdot\Delta T\cdot\sigma_{10,x}, 1.5\cdot\Delta T\cdot\sigma_{10,y}\right) \\ U\left(-1.5\cdot\Delta T\cdot\sigma_{10,x}, 1.5\cdot\Delta T\cdot\sigma_{10,z}\right) \end{bmatrix}$	$\boldsymbol{\varepsilon}_{D,10} = \begin{bmatrix} \delta(0) \\ \delta(0) \\ \delta(0) \end{bmatrix}$

Where ΔT depicts the window time from the RPE requirement.

- **PDE:**

By definition in [AD2] table B-4, a Uniform temporal distributed random variable does not contribute to the PDE error index. Additionally the ensemble distribution does not influence the contribution. Hence the PES reduces in every evaluation type to

$$\boldsymbol{\varepsilon}_{D,10,SI} = \begin{bmatrix} \delta(0) \\ \delta(0) \\ \delta(0) \end{bmatrix} \qquad \text{Eq 5-4}$$

6 Pointing Error Evaluation (AST-4)

This chapter summarizes the final pointing error results for the analysed pointing error indices of the PointingSat example according to AST-4 in [AD1], where applicable

The global frequency evaluation bandwidth used in PEET for all scenarios of the PointingSat example ranges from 10^{-5} Hz to 10^{3} Hz with a resolution of 1000 frequency points.

The selected PES for each error index are depicted in Table 6-1. The bandwidth is chosen in each scenario according to the computed necessary bandwidth by PEET. Note that PES 3, 5, 6, 7, 15 and 16 have been implemented twice in the PEET model. Once in the platform.knowledgeErr container and once in the platform.performanceErr container. This is easily possible with the copy and paste functionality in PEET. The reason is that for the knowledge error budget, the attitude knowledge error shall not be transferred through the AOCS control feedback loop.

Table 6-1: PES selection pes error index

	PES Number																	
	1	**2**	**3**	**4**	**5**	**6**	**7**	**8**	**9**	**10**	**11**	**12**	**13**	**14**	**15**	**16**	**17**	**18**
AKE	-	-	x	-	x	x	x	-	-	-	-	-	-	-	x	x	-	-
APE	x	x	x	x	x	x	x	x	x	x	x	x	x	x	x	x	x	x
PDE	x	x	x	x	x	x	x	x	x	x	x	x	x	x	x	x	x	x
RPE	x	x	x	x	x	x	x	x	x	x	x	x	x	x	x	x	x	x
WPD	x	x	x	x	x	x	x	x	x	x	x	x	x	x	x	x	x	x
WPR	x	x	x	x	x	x	x	x	x	x	x	x	x	x	x	x	x	x

The results computed with PEET are summarized in sections 6.1 through 6.6.

6.1 Scenario 1: APE

Table 6-2 and Table 6-3 summarize the overall results for the total error block for the APE requirement. The PDFs are split in time-constant, time-random and total figures and depicted in Figure 6-1 to Figure 6-3. The splitting of the results in the different ensemble domains is depicted in Table 6-4.

Table 6-2: Pointing APE budget

					APE											
PEC Name	Level	Output Unit	Domain	Value Type	Time Constant Error				Time Random Error				Total Error			
					x	y	z	LOS	x	y	z	LOS	x	y	z	LOS
Total Error	0	"	E1 AssemblyLaunch	Budget	60,95	44,23	33,91	51,3					60,95	44,23	33,91	51,3
			E2 EquipNoise	Budget	0,00001257	0	0,00000544	0,00000544	33,62	33,62	5,747	34,1	33,62	33,62	5,747	34,1
			E3 ExtEnvironment	Budget	0,6944	0,463	0,2315	0,5176	32,19	23,52	15,47	26,81	32,89	23,98	15,7	27,33
			E4 StatKeepingMan	Budget	0,006828	0,00569	0,006259	0,008459	33,2	27,67	30,44	41,13	33,21	27,67	30,44	41,14
			overall	Budget	61,22	44,49	34,12	51,62	92,33	79,47	43,17	89,68	139,9	115,9	72,5	131,8
				Requirement												150
				Requirement ID												Req_APE
interfacePEC	1	"	E1 AssemblyLaunch	Budget	58,99	42,16	31,39	48,53					58,99	42,16	31,39	48,53
			E3 ExtEnvironment	Budget	0,6944	0,463	0,2315	0,5176	24,73	18,42	12,08	21,07	25,42	18,89	12,31	21,59
			overall	Budget	58,85	42,23	31,43	48,63	24,74	18,41	12,09	21,05	75,12	54,22	38,98	62,84
				Requirement												
				Requirement ID												
payloadPEC	1	"	E2 EquipNoise	Budget	0	0	0	0	0,01123	0,01123	0,004272	0,01199	0,01123	0,01123	0,004272	0,01199
			E3 ExtEnvironment	Budget					1,196	1,559	1,6	2,234	1,196	1,559	1,6	2,234
			overall	Budget	0	0	0	0	1,208	1,571	1,604	2,245	1,208	1,571	1,604	2,245
				Requirement												
				Requirement ID												
platformPEC	1	"	E1 AssemblyLaunch	Budget	7,976	7,976	6,979	10,25					7,976	7,976	6,979	10,25
			E2 EquipNoise	Budget	0,00001252	0	0,000005364	0,000005364	33,61	33,61	5,742	34,09	33,61	33,61	5,742	34,09
			E3 ExtEnvironment	Budget	0,000004098	0,000006186	0,000009533	0,00001037	8,551	5,56	2,755	6,148	8,551	5,56	2,755	6,148
			E4 StatKeepingMan	Budget	0,006828	0,00569	0,006259	0,008459	33,2	27,67	30,44	41,13	33,21	27,67	30,44	41,14
			overall	Budget	7,983	7,982	6,985	10,26	70,44	62,63	35,92	72,17	78,13	70,37	42,83	81,15
				Requirement												
				Requirement ID												

Table 6-3: Overall results of APE requirement

	x-Axis [arcsec]	y-Axis [arcsec]	z-Axis [arcsec]	LoS [arcsec]
Time-constant	61.22	44.49	34.12	51.62
Time-random	92.33	79.47	43.17	89.68
Total	139.9	115.9	72.5	131.8

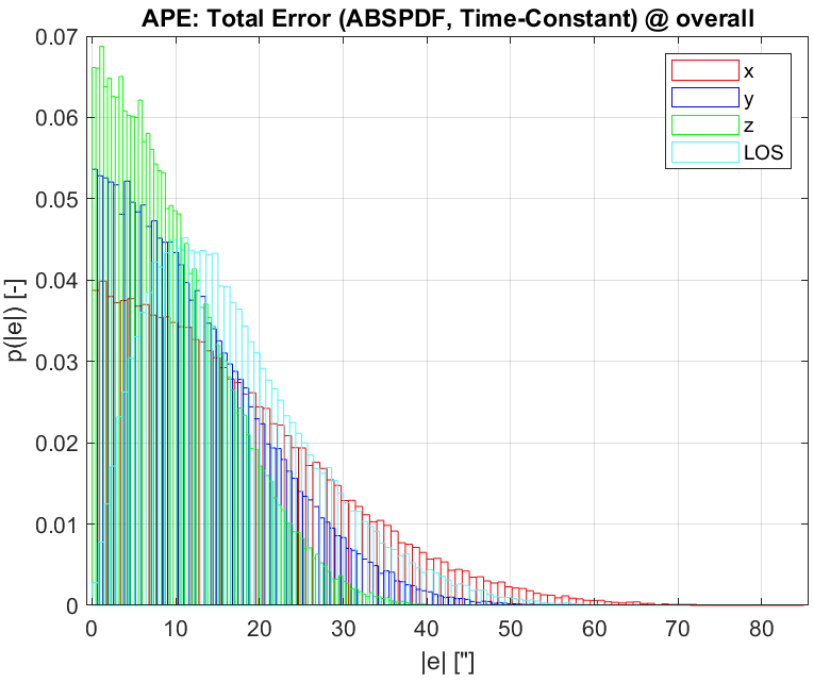

Figure 6-1: Overall PDF plot of time-constant part

Figure 6-2: Overall PDF plot of time-random part

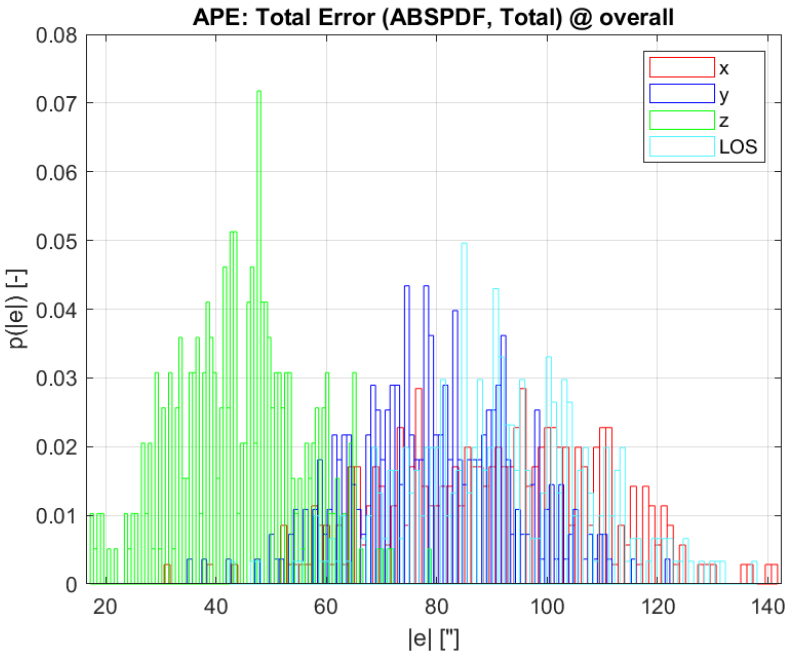

Figure 6-3: Overall PDF plot of total error

Table 6-4: Ensemble dependent results of APE requirement

	Ensemble Domain	x-Axis [arcsec]	y-Axis [arcsec]	z-Axis [arcsec]	LoS [arcsec]
Time-constant	Assembly & Launch	60.95	44.23	33.91	51.3
	Equipment Noise	1.257×10^{-5}	0	5.44×10^{-6}	5.44×10^{-6}
	Ext. Environment	0.6944	0.463	0.2315	0.5176
	Station Keeping	6.8×10^{-3}	5.69×10^{-3}	6.26×10^{-3}	8.46×10^{-3}
Time-random	Assembly & Launch	0	0	0	0
	Equipment Noise	33.62	33.62	5.747	34.1
	Ext. Environment	32.19	23.52	15.47	26.81
	Station Keeping	33.2	27.67	30.44	41.13
Total	Assembly & Launch	60.95	44.23	33.91	51.3
	Equipment Noise	33.62	33.62	5.747	34.1
	Ext. Environment	32.89	23.98	15.7	27.33
	Station Keeping	33.21	27.67	30.44	41.14

It can be seen that the overall pointing errors do not follow a Gaussian distribution. However, PEET computes the level of confidence (LoC) based on the actual distributions and thus ensures precise evaluation.

The probability density function (PDF) of the azimuth and elevation pointing errors are shown in . This is computed via a post-processing script in PEET that uses directly the accurately modelled pointing behaviour with its underlying PDFs.

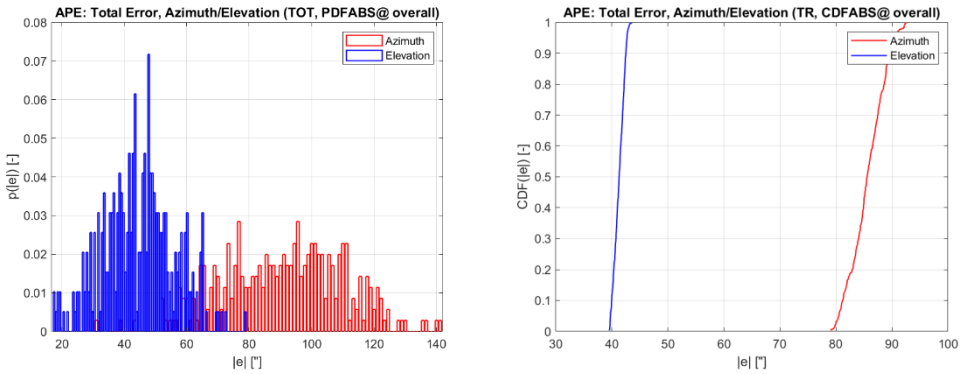

Figure 6-4: Overall PDF and CDF for APE azimuth and elevation errors

Result summary

The APE requirement is reached with a margin of 18.8 arcsec. The main contributors can be identified due to the analysis with PEET as the time-constant PES from the “Assembly & Launch” ensemble-domain. However as the requirements are met with sufficient margin there is no need to increase the performance of any spacecraft part.

6.2 Scenario 2: RPE

Table 6-5 summarizes the results for the RPE requirements. As the level of confidence is different for each ensemble-domain, it is not useful to depict an overall PDF.

Table 6-5: Pointing RPE budget

PEC Name	Level	Output Unit	Domain	Value Type	RPE				Description
					Total Error				
					x	y	z	LOS	
Total Error	0	''	E1 AssemblyLaunch	Budget	0	0	0	0	
			E2 EquipNoise	Budget	0,3962	0,3967	0,2915	0,5226	
			E3 ExtEnvironment	Budget	1,996	1,996	1,996	2,823	
			E4 StatKeepingMan	Budget	0,9722	0,8102	0,8912	1,204	
			overall	Budget	3,364	3,203	3,179	4,55	
				Requirement				8	
				Requirement ID				Req_RPE	
interfacePEC	1	''	E1 AssemblyLaunch	Budget	0	0	0	0	
			E3 ExtEnvironment	Budget	1,996	1,996	1,996	2,822	
			overall	Budget	1,996	1,996	1,996	2,822	
				Requirement					
				Requirement ID					
payloadPEC	1	''	E2 EquipNoise	Budget	0,00718	0,00718	0,002325	0,007523	
			E3 ExtEnvironment	Budget	0,00182	0,00236	0,002435	0,003645	
			overall	Budget	0,009	0,00954	0,00476	0,01117	
				Requirement					
				Requirement ID					
platformPEC	1	''	E1 AssemblyLaunch	Budget	0	0	0	0	
			E2 EquipNoise	Budget	0,3986	0,3957	0,2911	0,5228	
			E3 ExtEnvironment	Budget	0,00146	0,00146	0,0007027	0,001665	
			E4 StatKeepingMan	Budget	0,9722	0,8102	0,8912	1,204	
			overall	Budget	1,372	1,207	1,183	1,729	
				Requirement					
				Requirement ID					

Result summary

The requirement of 8 arcsec for the LoS RPE is fulfilled with a margin of almost 100%. The ensemble domain “External Environment” can be identified as the main contributor.

6.3 Scenario 3: WPD

Table 6-6 summarizes the results for the RPE requirements. As the level of confidence is different for each ensemble-domain, it is not useful to depict an overall PDF.

Table 6-6: Pointing WPD budget

					WPD				
PEC Name	Level	Output Unit	Domain	Value Type	Total Error				Description
					x	y	z	LOS	
Total Error	0	"	E1 AssemblyLaunch	Budget	0	0	0	0	
			E2 EquipNoise	Budget	1,309	1,311	0,9209	1,695	
			E3 ExtEnvironment	Budget	0,009277	0,01041	0,009126	0,01471	
			E4 StatKeepingMan	Budget	1,955	1,629	1,792	2,421	
			overall	Budget	3,273	2,95	2,722	4,131	
				Requirement				5	
				Requirement ID				Req_WPD	
interfacePEC	1	"	E1 AssemblyLaunch	Budget	0	0	0	0	
			E3 ExtEnvironment	Budget	0,002262	0,001642	0,0007472	0,001799	
			overall	Budget	0,002262	0,001642	0,0007472	0,001799	
				Requirement					
				Requirement ID					
payloadPEC	1	"	E2 EquipNoise	Budget	0,00002924	0,00002923	0,00001508	0,00003289	
			E3 ExtEnvironment	Budget	0,006297	0,008188	0,008436	0,01263	
			overall	Budget	0,006327	0,008217	0,008451	0,01266	
				Requirement					
				Requirement ID					
platformPEC	1	"	E1 AssemblyLaunch	Budget	0	0	0	0	
			E2 EquipNoise	Budget	1,317	1,307	0,9192	1,696	
			E3 ExtEnvironment	Budget	0,005033	0,005037	0,002429	0,005762	
			E4 StatKeepingMan	Budget	1,955	1,629	1,792	2,421	
			overall	Budget	3,277	2,941	2,713	4,123	
				Requirement					
				Requirement ID					

Result summary

The requirement of 5 arcsec for the LoS WPD is fulfilled with a sufficient margin. Here, the ensemble domain “station keeping manoeuvre” is the main contributor, accounting for over 50% of the total budget.

6.4 Scenario 4: WPR

Table 6-7 summarizes the results for the RPE requirements. As the level of confidence is different for each ensemble-domain, it is not useful to depict an overall PDF.

Table 6-7: Pointing WPR budget

					WPR				
PEC Name	Level	Output Unit	Domain	Value Type	Total Error				Description
					x	y	z	LOS	
Total Error	0	"	E1 AssemblyLaunch	Budget	0	0	0	0	
			E2 EquipNoise	Budget	0,1492	0,1496	0,1509	0,2276	
			E3 ExtEnvironment	Budget	1,996	1,996	1,996	2,822	
			E4 StatKeepingMan	Budget	2,951	2,459	2,705	3,656	
			overall	Budget	5,096	4,604	4,852	6,706	
				Requirement				7	
				Requirement ID				Req_WPR	
interfacePEC	1	"	E1 AssemblyLaunch	Budget	0	0	0	0	
			E3 ExtEnvironment	Budget	1,996	1,996	1,996	2,822	
			overall	Budget	1,996	1,996	1,996	2,822	
				Requirement					
				Requirement ID					
payloadPEC	1	"	E2 EquipNoise	Budget	0,007173	0,007171	0,002318	0,007518	
			E3 ExtEnvironment	Budget	0,00009402	0,0001222	0,0001259	0,0001885	
			overall	Budget	0,007267	0,007293	0,002444	0,007706	
				Requirement					
				Requirement ID					
platformPEC	1	"	E1 AssemblyLaunch	Budget	0	0	0	0	
			E2 EquipNoise	Budget	0,15	0,1489	0,1508	0,2278	
			E3 ExtEnvironment	Budget	0,00001159	0,00001163	0,000005611	0,0000133	
			E4 StatKeepingMan	Budget	2,951	2,459	2,705	3,656	
			overall	Budget	3,101	2,608	2,856	3,884	
				Requirement					
				Requirement ID					

Result summary

The requirement of 7 arcsec for the LoS WPR is fulfilled, albeit with a tight margin. The main contributors are the ensemble domains “external environment” and “station keeping manoeuvre”. A sensible next step would be to analyse the individual PECs in these ensemble domain to identify the driving contributors. This would then allow to implement targeted mitigation measures.

6.5 Scenario 5: PDE

Table 6-8 summarizes the results for the total error block for the PDE requirement and the PDF is shown in Figure 6-5. The splitting of the results in the different ensemble domains is depicted in .

Table 6-8: Pointing PDE budget

					PDE				
PEC Name	Level	Output Unit	Domain	Value Type	Total Error				Description
					x	y	z	LOS	
Total Error	0	"	E1 AssemblyLaunch	Budget	0	0	0	0	
			E2 EquipNoise	Budget	66,2	65,7	10,5	65,86	
			E3 ExtEnvironment	Budget	6,83	5,41	3,55	5,811	
			E4 StatKeepingMan	Budget	0	0	0	1,46E-12	
			overall	Budget	66,6	66	11,1	66,05	
				Requirement				50	
				Requirement ID				Req_PDE	
interfacePEC	1	"	E1 AssemblyLaunch	Budget	0	0	0	0	
			E3 ExtEnvironment	Budget	5,62	3,76	1,86	4,195	
			overall	Budget	5,62	3,76	1,86	4,195	
				Requirement					
				Requirement ID					
payloadPEC	1	"	E2 EquipNoise	Budget	0	0	0	8,35E-16	
			E3 ExtEnvironment	Budget	2,08	2,72	2,82	3,166	
			overall	Budget	2,08	2,72	2,82	3,166	
				Requirement					
				Requirement ID					
platformPEC	1	"	E1 AssemblyLaunch	Budget	0	0	0	0	
			E2 EquipNoise	Budget	65,6	65,6	10,6	65,76	
			E3 ExtEnvironment	Budget	2,63	2,62	1,28	2,661	
			E4 StatKeepingMan	Budget	0	0	0	1,46E-12	
			overall	Budget	65,1	66,2	10,7	66,27	
				Requirement					
				Requirement ID					

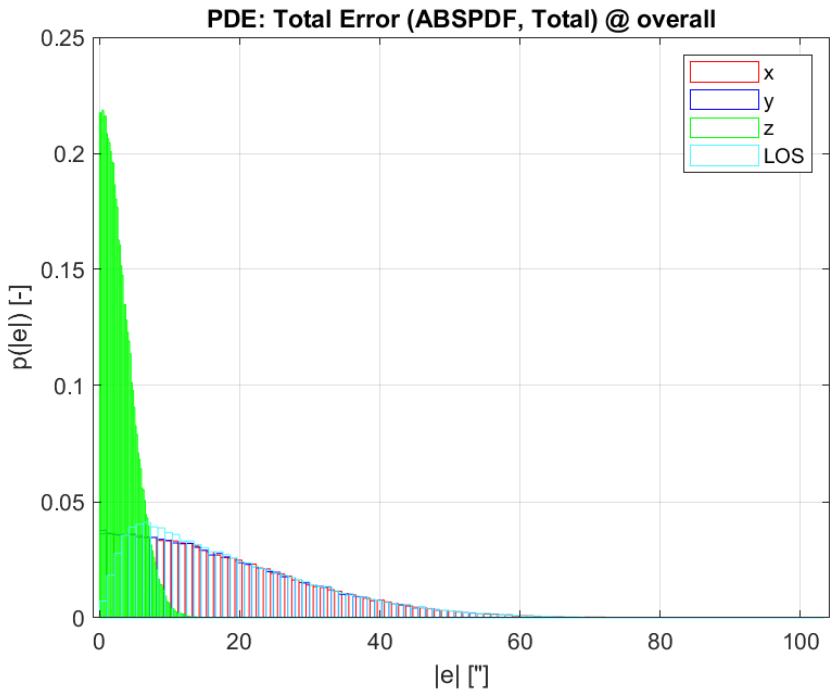

Figure 6-5: Overall PDF plot of total error

Result summary

The PDE LoS requirement of 50 arcsec is exceeded by around 30%. The main driver can be identified from Table 6-8 as the time-random errors of the “Equipment Noise” ensemble-domain. That means that for example reduced cryocooler microvibrations can improve the performance and help to stay within the requirements.

6.6 Scenario 6: AKE

This scenario is defined by a spectral requirement and therefore PEET does not depict the mean value and standard deviation as they are not of interest. Furthermore the PDF of random processes (which are the only allowed error sources for spectral requirements) is defined as Gaussian and therefore not shown either. The PSD however is of interest and shown for the AKE scenario in Figure 6-6. Accordingly, the tabular report generated by PEET only states whether the requirement is fulfilled or not (“Requirement Compliance”). The table contains links to the corresponding PSD plots, where the budget and the requirement are shown in a magnitude over frequency plot

Table 6-9: Pointing AKE budget

PEC Name	Level	Output Unit	AKE					
			Requirement Compliance			Requirement ID		
			x	y	z	x	y	z
Total Error	0	"	marginal	marginal	yes	Req_AKE_x	Req_AKE_y	Req_AKE_z
interfacePEC	1	"	N/A	N/A	N/A			
payloadPEC	1	"	N/A	N/A	N/A			
platformPEC	1	"	N/A	N/A	N/A			

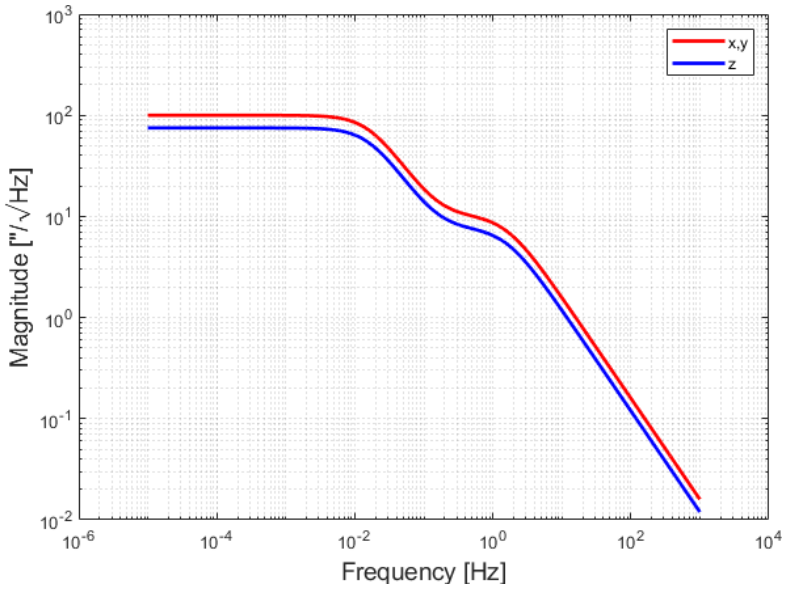

Figure 6-6: PSD at total error block for AKE spectral requirement

Results summary

Figure 6-7 to Figure 6-9 show the comparison of the requirement PSD with the PSD from the PEET output for each axis. It can be seen that the requirement is met for all three axes. However there is little margin in the frequency range from 0.01 Hz to 0.02 Hz. Hence special focus shall be given for changes regarding this frequency spectrum.

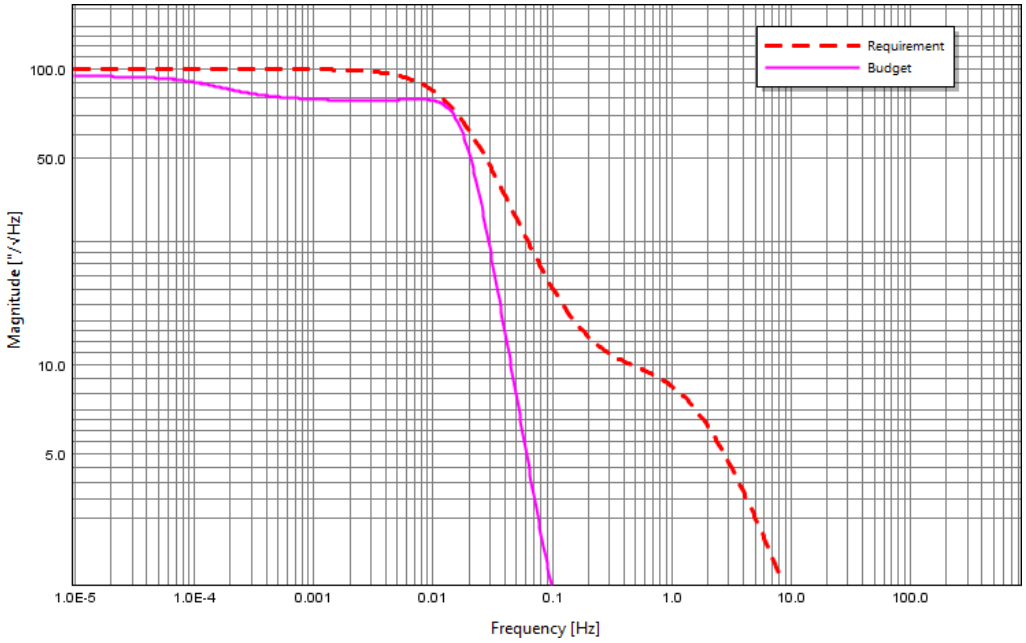

Figure 6-7: X-Axis output PSD compared with requirement

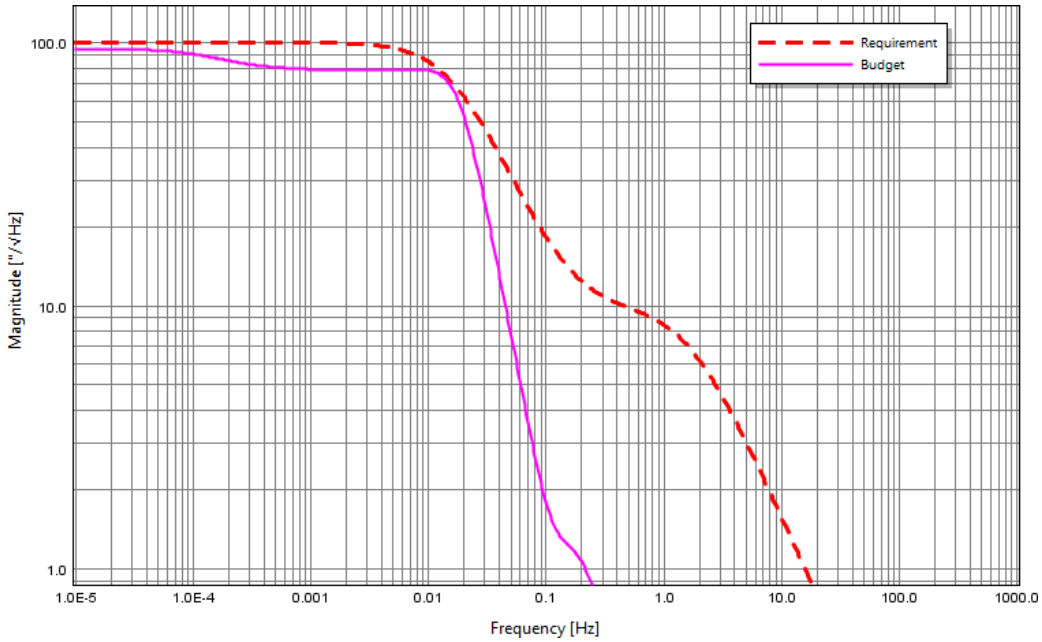

Figure 6-8: Y-Axis output PSD compared with requirement

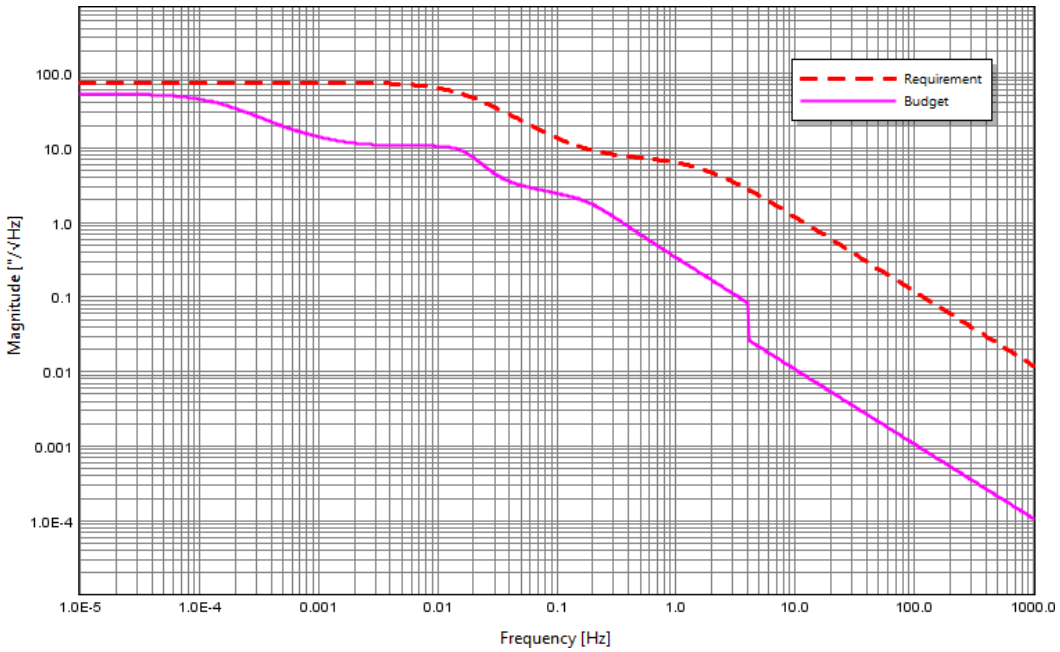

Figure 6-9: Z-Axis output PSD compared with requirement

7 Remarks

It is important to note that above collection of PES is not intended to be exhaustive. Not in a sense that all possible error sources are covered and not in sense that all possible contributors to a single PES are set (e.g. PES 4 could comprise an additional torque noise, PES 7 could have an additional ensemble distribution of the power spectrum, PES 14 could have a non-zero mean value, etc.).

The intention of the PES description is simply to cover all different kinds of error source representations.

The same is true for the realization of the system transfer models which should only show the basic predefined possibilities of PEET. Most of them are very simplified approximations of the real system behaviour only and not optimized to represent a ‘matching system’. However, in PEET it is up to the user define own system block types with arbitrary complexity of the models (by extending the existing PEET Matlab classes)